Chapter 10
Electricity from Microbial Fuel Cells

Jun Li, Wei Yang, Biao Zhang, Dingding Ye, Xun Zhu and Qiang Liao

1 Introduction

The development and implementation of renewable energy resources is an effective approach to cope with global energy and pollution issues. Microbial fuel cell (MFC) technology has the promise to produce electrical energy and treat wastewater simultaneously because it converts the chemical energy contained in wastewater to electricity using electrochemically active bacteria (EAB) [1]. A schematic diagram of an MFC is shown in Fig. 1. In a typical MFC, electrons are produced from the degradation of organic matter by the metabolism of an EAB biofilm attached to the anode. The electrons are then transferred to the cathode through an external circuit where they are combined with protons and finally electron acceptors (e.g., oxygen) to close the circuit [2]. Unlike the combustion process, the oxidation and reduction reactions occur on the anode and cathode separately, requiring anaerobic anode conditions to keep the EAB from oxygen or any other terminal acceptors for electricity generation [3]. When acetate and oxygen are used as reactants (fuels) the electrode reactions at pH 7 are as follows:

Anode reaction:

$$CH_3COO^- + 4H_2O \rightarrow 2HCO_3^- + 9H^+ + 8e^- \quad E_a^0 = -0.300$$

J. Li (✉) · W. Yang · B. Zhang · D. Ye · X. Zhu · Q. Liao
Key Laboratory of Low-Grade Energy Utilization Technologies and Systems, Chongqing University, Chongqing 400030, China
e-mail: lijun@cqu.edu.cn

J. Li · W. Yang · B. Zhang · D. Ye · X. Zhu · Q. Liao
Institute of Engineering Thermophysics, Chongqing University, Chongqing 400030, China

Q. Liao et al. (eds.), *Bioreactors for Microbial Biomass and Energy Conversion*, Green Energy and Technology, https://doi.org/10.1007/978-981-10-7677-0_10

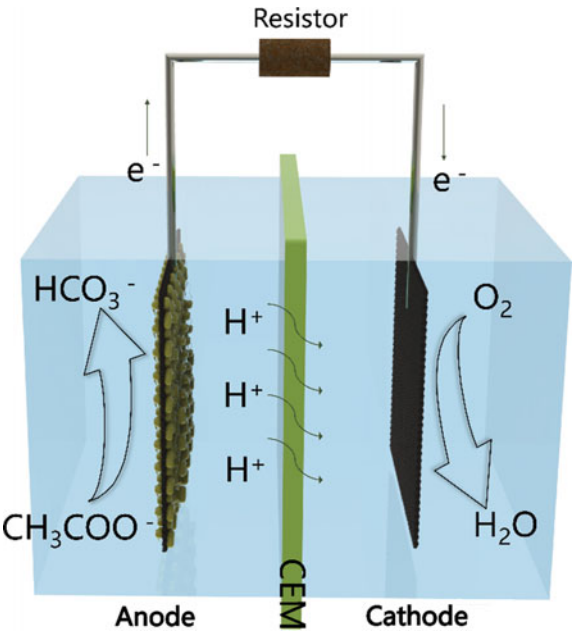

Fig. 1 Schematic diagram of an MFC

Cathode reaction:

$$2O_2 + 8e^- + 8H^+ \rightarrow 4H_2O \quad E_c^0 = 0.805\,\mathrm{V}$$

Overall reaction:

$$CH_3COO^- + 2O_2 \rightarrow 2HCO_3^- + H^+ \quad E^0 = 1.105\,\mathrm{V}$$

Based on the reaction above, the substrate is decomposed into bicarbonate and oxygen is reduced to water. When wastewater is fed into MFCs, the organic/inorganic matters can be degraded, providing wastewater treatment and energy recovery in the form of electricity.

Many efforts have been made to improve the capacity of MFC technology for waste treatment and power generation. Many organic matters such as acetate, glucose, butyrate, and lactate (Table 1), have been used as substrates for MFCs and this has demonstrated the feasibility of recovering electricity from different organic matters [4]. To simulate and verify the in situ treatment of MFC technology, some prototypes have been tested using brewery wastewater, landfill wastewater, and starch processing wastewater under continuous or batch feed conditions (Table 1). Liu et al. reported an MFC capable of producing electricity from domestic wastewater. The MFC generated a maximum power output of 26 mW/m^2 while

Table 1 Different substrates used in microbial fuel cells (MFCs)

Type of substrate	Concentration	Source inoculum	Type of MFC (with electrode surface area and/or cell volume)	References
Glucose	6.7 mM	Mixed bacterial culture maintained on sodium acetate for 1 year	One-chamber air-cathode MFC (12 mL) with non wet proofed carbon cloth as anode (2 cm^2) and wet proofed carbon cloth as cathode (7 cm^2)	[7]
Acetate	1 g/L	Pre-acclimated bacteria from MFC	Cube shaped one-chamber MFC with graphite fiber brush anode (7170 m^2/m^3 brush volume)	[8]
Lactate	18 mM	Pure culture of *S. oneidensis* MR-1	Two-chambered MFC with graphite felt electrode (20 cm^2)	[9]
Domestic wastewater	600 mg/L	Anaerobic sludge	Two-chambered mediator-less MFC with plain graphite electrode (50 cm^2)	[10]
Brewery wastewater	2240 mg/L	Full strength brewery wastewater	One-chamber air-cathode MFC with non-wet proofed carbon cloth as anode (7 cm^2) and wet proofed carbon cloth containing Pt as cathode	[11]
Beer brewery wastewater	600 mg/L	Anaerobic mixed consortia	One-chamber air-cathode MFC with carbon fibers as anode	[12]
Starch processing wastewater	4852 mg/L COD	Starch processing wastewater	One-chamber air-cathode MFC with carbon paper anode (25 cm^2)	[13]
Landfill leachate	6000 mg/L	Leachate and sludge	Two-chambered MFC with carbon veil electrode (30 cm^2)	[14]
Azo dye with glucose	300 mg/L	Mixture of aerobic and anaerobic sludge	One-chamber air-cathode MFC with carbon paper anode (36 cm^2)	[15]
Synthetic wastewater	510 mg/L	Anaerobic culture from a preexisting MFC	Dual chamber MFC with stainless tell as anode (170 cm^2) and graphite rods as cathode (150 cm^2)	[16]

removing 80% of the chemical oxygen demand (COD) in the wastewater [2]. Many studies have focused on MFC scale-up and practical applications. MFC studies have typically been conducted in reactors with small volumes ranging from several

microliters to liters. These reactors are suitable for obtaining basic information but for practical wastewater treatment, the goal is to develop a scalable technology for large-scale implementation. The first large-scale MFC test was performed at Foster's brewery in Yatala by the Advanced Water Management Center at the University of Queensland. This study used a reactor consisting of 12 modules, each 3 m high, with a total volume of approximately 1 m^3 [5]. The goal is for the electricity recovered from wastewater to at least partially cover the cost of the wastewater treatment process. To date, the electrical power production has been increased by five- to sixfolds and improvements continue to be made [5]. Novel approaches have been reported to improve MFC performance, either by optimizing the MFC structure or exploring cost-efficient and high performance electrode materials. To improve the cathode performance while reducing cost, a stainless steel mesh-based (SSM) cathode and inexpensive carbon catalysts were proposed to replace the conventional expensive platinum-based (Pt) system for MFC applications [6].

Although significant improvements have been achieved, challenges remain in scale-up and practical applications. A major obstacle for MFC application is the low amount of electricity generation. This is mainly affected by four factors: (1) the biofilm's activity to oxidize the substrate of the anode, (2) the low efficiency of the electron transfer between the biofilm and the anode, (3) the slow oxygen reduction reaction (ORR) at the cathode, and (4) the high internal ohmic resistance. Many methods have been tested to enhance MFC performance. These include: exploiting three-dimensional (3D) open porous anode materials, preparing novel ORR catalysts, and optimizing the reactor architecture. Another major limitation is the high fabrication cost of MFCs. In typical MFCs, the most commonly used ORR catalyst is platinum and its alloys. The anode materials are carbon cloth or carbon paper. The costs for both of these materials are high, especially for large-scale wastewater treatment applications. In addition, the procedure for fabricating electrodes is complex and labor intensive; this also increases the cost of MFCs. For example, the MFC cathode is usually prepared by brushing or spraying catalyst inks onto the supporting carbon materials, leading to an additional cost in MFC applications [6, 17]. These problems are being addressed by research on high-efficiency materials and optimized MFC electrode designs. The goal is the development of a scalable technology for treating different types of wastewater and simultaneous energy recovery.

This chapter (1) details the fundamental principles of MFCs, (2) reviews the electrode materials and construction methods, (3) provides an overview of MFC architecture, (4) discusses the MFC stack and the feasibility in practical power generation, and (5) reviews the various applications of MFC technology.

2 Fundamental Principles of MFCs

2.1 Voltage and Current

A working MFC usually produces an operating voltage (U) of $\sim$0.5 V, which is a function of external resistance (R_{ex}) and current (I). The relationship is as follows:

$$U = IR_{ex} \tag{1}$$

Therefore, the current can be calculated from the measured voltage drop across the external resistance as $I = U/R_{ex}$. The highest voltage, which is produced in an open-circuit condition, is open-circuit voltage (OCV).

The theoretical maximum voltage (reversible voltage) that can be generated from an MFC is limited by thermodynamics, which can be predicted by the Nernst equation:

$$E_{mef} = \mathrm{E}^0 - \frac{RT}{nF}\ln\frac{[\text{products}]^{\mathrm{p}}}{[\text{reactants}]^{\mathrm{r}}} \tag{2}$$

where E_{mef} is the maximum electromotive force, E^0 is the standard cell electromotive force, R is the gas constant (8.31447 J/mol K), T is the absolute temperature (K), n is the transferred electron number, and F = 96,485 C/mol is the Faraday's constant. According to the International Union of Pure and Applied Chemistry (IUPAC) convention, all of the reaction equations are expressed in the direction of a reduction reaction, so that the production and reactants are the reduced and oxidized species respectively. E° is calculated based on hydrogen under standard conditions (at 298 K, chemical concentration of 1 M for liquid and 1 bar for gases), which is defined as E° (H_2) = 0, referred to as the normal hydrogen electrode (NHE).

Based on these principles, the electrode potential and voltage generation can be determined. In an MFC system, the bacteria need to be operated in neutral pH conditions. The ORR reaction can be described as:

$$1/2\mathrm{O_2} + 2\mathrm{H^+} + 2\mathrm{e^-} \rightarrow \mathrm{H_2O},\ E^0(\mathrm{O_2}) = 1.229\ \mathrm{V}$$

Then, the cathode potential (E_c) at pH = 7 can be calculated as [18]:

$$E_c = E^0 - \frac{RT}{nF}\ln\frac{1}{[\mathrm{O_2}]^{1/2}[\mathrm{H^+}]^2}$$

$$E_c = 1.229\ \mathrm{V} - \frac{(8.31\ \mathrm{J/mol\ K})(298.15\ \mathrm{K})}{(2)(96{,}485\ \mathrm{C/mol})}\ln\frac{1}{[0.2\ \mathrm{mol/L}]^{1/2}[10^{-7}\ \mathrm{mol/L}]^2}$$
$$= 0.805\ \mathrm{V}$$

For an MFC using acetate as the substrate, the HCO_3^-/Ac can be expressed as:

$$2HCO_3^- + 9H^+ + 8e^- \rightarrow 4H_2O + CH_3COO^-$$

For acetate E^0 (acetate) = 0.187 V, with a concentration of 1 g/L, a neutral pH = 7 and a bicarbonate concentration of HCO_3^- = 5 mM, the anode potential (E_a) can be calculated as [18]:

$$E_a = E^0 - \frac{RT}{nF} \ln \frac{[CH_3COO^-]}{[HCO_3^-]^2[H^+]^9}$$

$$E_a = 0.187\,\text{V} - \frac{\left(\frac{8.31\text{J}}{\text{mol}} \cdot \text{K}\right)(298.15\,\text{K})}{(8)\left(96,485\frac{\text{C}}{\text{mol}}\right)} \ln \frac{1}{\left[0.005\frac{\text{mol}}{\text{L}}\right]^2\left[10^{-7}\frac{\text{mol}}{\text{L}}\right]^9} = -0.300\text{V}$$

The highest cell voltage that can be generated from an MFC is the difference between the anode and cathode potentials:

$$E = E_c - E_a \tag{3}$$

Therefore, an MFC using acetate as the substrate and oxygen as the terminal electron acceptor can obtain a maximum voltage output of 0.805 V – (–0.300 V) = 1.105 V. However, in practical applications, the voltage output of the air-cathode MFCs is much lower than this value. This can be attributed to two aspects: the first is the voltage loss caused by activation losses, ohmic losses, and mass transfer losses during the operation. The second is the inefficient ORR through a two-electron pathway (E_c = 0.328 V), compared to a four-electron pathway (E_c = 0.805 V).

2.2 Electricity Generation and Energy Recovery

In an MFC, power is calculated from the measured voltage and current across the external load as:

$$P = IU \tag{4}$$

The current produced by an MFC can be obtained by measuring the voltage drop across the external resistor using $I = U/R_{ex}$, thus, the power can be expressed as a function of U and R_{ex}:

$$P = \frac{U^2}{R_{ex}} \tag{5}$$

Based on the equation $I = U/R_{ex}$, power also can be expressed in terms of the calculated current as:

$$P = I^2 R_{ex} \tag{6}$$

2.2.1 Power Density

To evaluate the power output generated from an MFC with a specific architecture, the power density can be calculated based on the electrode surface area or the reactor volume. Thus the power density can be categorized into surface specific power density and volumetric power density.

Surface specific power density is the power output normalized by the electrode surface area:

$$P_a = \frac{U^2}{A_a R_{ex}} \text{ or } P_c = \frac{U^2}{A_c R_{ex}} \tag{7}$$

where P_a and P_c are the power density based on the anode and cathode surface area, respectively. A_a and A_c are the effective areas of the anode and cathode, which can be the specific surface area or geometric area. In an MFC with a membrane or separator, power density can also be calculated based on the membrane/separator area (A_m). Volumetric power density, used to evaluate the power output of a whole MFC system, is the power output normalized by the reactor volume. Volumetric power density can be expressed as:

$$P_V = \frac{U^2}{V R_{ex}} \tag{8}$$

where P_V is the volumetric power density (W/m^3) and V is the volume of the reactor (m^3).

2.2.2 Energy Recovery

The goal of MFC technology is to recover the energy contained in the wastewater. To evaluate the recovery efficiency of electrons from wastewater, coulombic efficiency (CE) is commonly used and it is defined as the fraction of coulombs recovered versus the total energy contained in the wastewater:

$$\mathrm{CE} = \frac{\text{Coulombs recovered}}{\text{Total coulombs in substrate}} \tag{9}$$

Coulombs can be calculated by integrating the current with the time; therefore, CE can be expressed as:

$$CE = \frac{M \int_0^t I dt}{FeV\Delta C} \tag{10}$$

where M is the molecular weight of substrate (g/mol), V is the volume of the liquid in the anode chamber (m^3), and ΔC is the substrate concentration (mol/L) change over a fed-batch cycle (t).

For an MFC system using complex substrates, CE can be obtained using COD as the measure of substrate concentration:

$$\mathrm{CE} = \frac{8 \int_0^t I dt}{FV\Delta COD} \tag{11}$$

where 8 is a constant for the COD, based on the molecular weight of oxygen (32 g/mol), and 4 is the electron transfer number per mol of oxygen.

2.3 *Polarization and Power Density Curves*

The polarization curve is a plot of current density versus voltage, which can be obtained by varying the external resistance while recording the current density and voltage values at each resistance (Fig. 2a). A typical polarization curve of an MFC is shown in Fig. 2b. The power density curve, as a function of current density, is usually shown along with the polarization curve. It is also commonly observed that

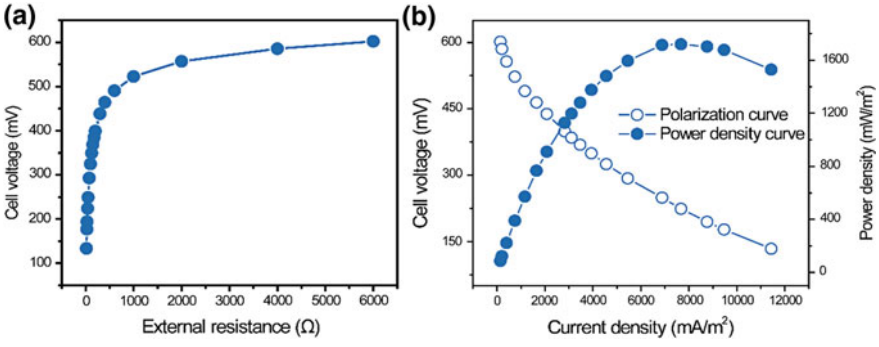

Fig. 2 Cell voltage as a function of external resistances (**a**), polarization curve, and power density curve of an MFC (**b**)

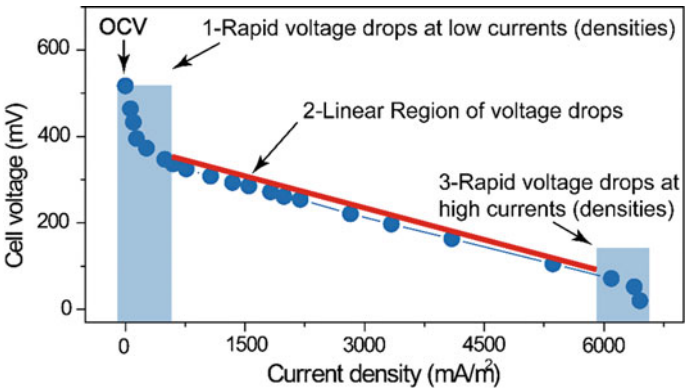

Fig. 3 Characteristics of a polarization curve, showing three types of voltage losses

a peak, called the maximum power density, appears at high current densities in the power density curve.

The OCV and the operation voltage of an MFC are always lower than the reversible voltage predicted by the Nernst equation. To analyze the voltage losses, the polarization curve can be divided into three regions: (1) a rapid voltage drop at low current densities; (2) a nearly linear decrease in voltage at medium current densities; and (3) a rapid voltage drop at high current densities (Fig. 3). The voltage losses are the result of electrode overpotentials, which are current dependent (overpotentials change with current densities). Electrode overpotentials are thought to arise from basic losses corresponding to three regions: (1) activation losses; (2) ohmic losses; and (3) mass transport losses.

(1) Activation losses are the energy losses incurred for driving the oxidation or reduction reactions, and for transferring electrons from the bacteria to the anode surface by the conductive nanowire, mediator, or terminal cytochrome on the cell surface [18]. Enhancing the electron transfer between anode and bacteria, using highly efficient cathode catalysts, and improving the anode biofilm metabolism activity for substrate oxidation would reduce the activation losses.
(2) Ohmic losses arise from the resistance of ion conduction in the solution and membrane and the flow of electrons through the electrodes and wires as well as their connection points. The ohmic losses can be reduced by decreasing the electrode spacing, removing the membrane or using a membrane with a high ion conductivity, increasing the solution conductivity, improving the electrode conductivity, and ensuring a good connection between the electrodes and connection wires.
(3) Mass transport losses arise from the insufficient transport of species to/from the electrode. At the anode, ensuring a sufficient substrate supply and proton removal is an effective approach for reducing mass transport losses. The limited proton removal within the biofilm can be a problem as it lowers the local pH of

biofilm and adversely affects the biofilm activity. Similarly, the limited proton supply for the ORR at the cathode can also increase the pH, which can lower the cathode potential and decrease the cathode performance.

2.4 *Electrochemical Analysis*

2.4.1 Electrochemical Impedance Spectroscopy (EIS)

EIS is commonly used for quantifying the internal resistance of MFCs. Generally, EIS tests are performed on a potentiostat by applying a sinusoidal signal with small amplitude on the working electrode. By changing the sinusoidal signal frequency over a wide range (typically from 100 kHz to 0.01 Hz), impedance spectra can be obtained for the MFC system. A Nyquist curve is plotted using the impedance spectra as the real impedance (Z_{re}) versus imaginary impedance (Z_{im}), as shown in Fig. 4. To obtain more detailed information about the component of the internal resistance, the impedance spectra usually needs to be fitted using an equivalent circuit by EIS software.

2.4.2 Voltammetry

Voltammetry is typically used to determine the redox potential of redox active matter. The information can be used to evaluate electrochemical activity of the biofilm and cathode catalysts. There are two types of voltammetry: linear sweep

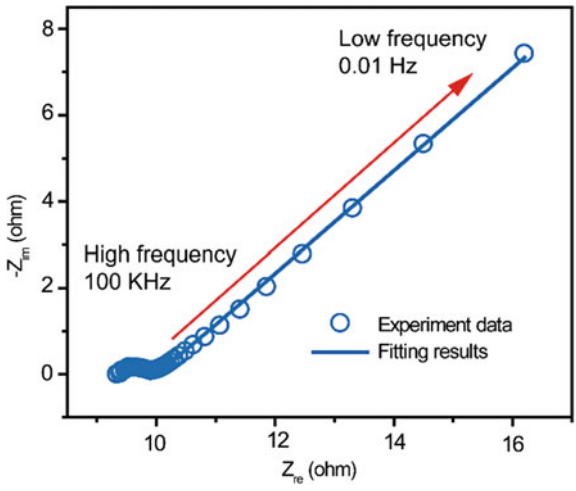

Fig. 4 Nyquist plots of an activated carbon cathode in a single-chamber MFC

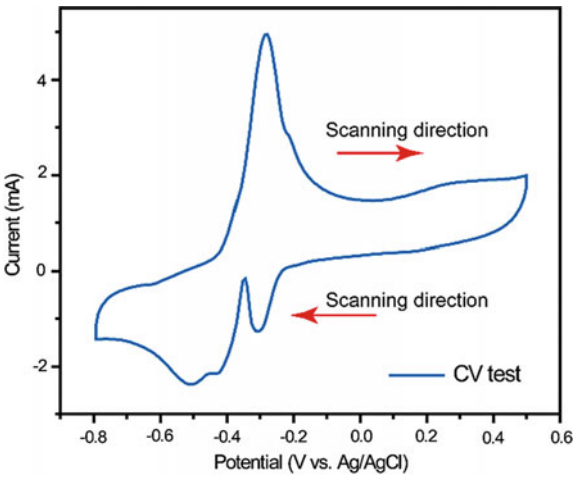

Fig. 5 Cyclic voltammetry of the anode of an MFC under turnover conditions

voltammetry (LSV) and cycle voltammetry (CV). In LSV tests, the potential of the working electrodes (anode or cathode) varies at a certain scan rate in one direction. For CV tests, the scan is conducted in one direction first and then continued in the reverse direction until the potential is returned to the start value (Fig. 5). In an MFC system, CV is the most commonly used method to determine the presence of electron shuttles or mediators produced by bacteria under non-turnover conditions and to determine the oxidation current of anode biofilm under turnover conditions. LSV is mainly applied to record the current response of the cathode under different potentials for the evaluation of the electrocatalytic activity of the ORR (Figs. 6 and 7).

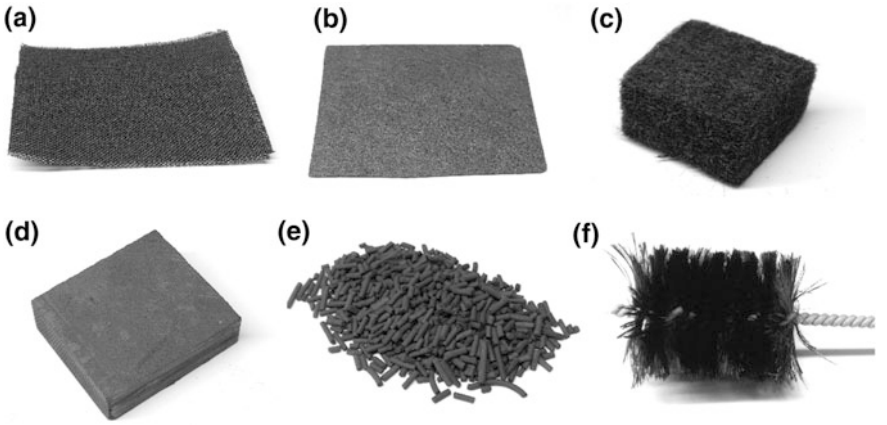

Fig. 6 Common anode materials used in MFCs: **a** carbon cloth, **b** carbon paper, **c** carbon felt, **d** graphite plate, **e** granular carbons, and **f** carbon brush

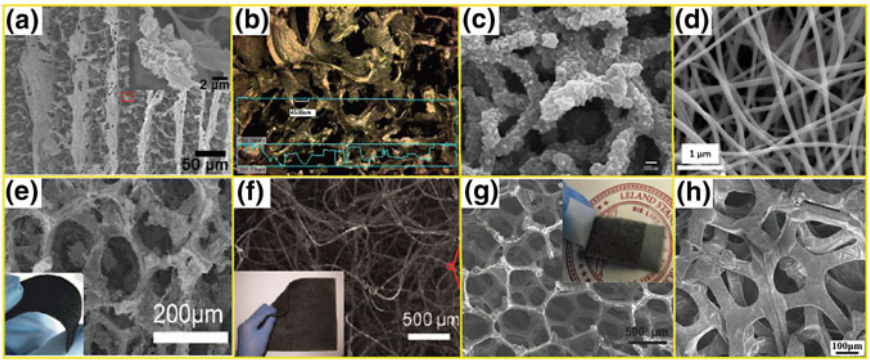

Fig. 7 3D porous anode derived from nanomaterials: **a** chitosan/vacuum-stripped graphene scaffolds (adapted and reprinted from [19], Copyright 2012, with permission from American Chemical Society), **b** 3D chitosan–carbon nanotube scaffolds (adapted and reprinted from [20], Copyright 2011, with permission from Elsevier), **c** CNT/PANI nanocomposite (adapted and reprinted from [21], Copyright 2007, with permission from Elsevier), **d** porous carbon nanofiber aerogel (adapted and reprinted from [22], Copyright 2016, with permission from Wiley), **e** graphene-coated nickel foam (adapted and reprinted from [23], Copyright 2013, with permission from Royal Society of Chemistry), **f** 3D carbon nanotube-textile (adapted and reprinted from [24], Copyright 2011, with permission from American Chemical Society), **g** graphene-sponge (adapted and reprinted from [25], Copyright 2012, with permission from Royal Society of Chemistry), and **h** polyaniline hybridized three-dimensional graphene (adapted and reprinted from [26], Copyright 2012, with permission from American Chemical Society)

3 Electrode and Separator Materials of MFCs

As discussed in Sect. 2.3, the power generation of an MFC depends on the rate of substrate degradation, bacterial growth and respiration rate on the anode, circuit resistance, ion mass transfer in the electrolyte, mass transfer of the cathode electron acceptor, reduction rate of the cathode electron acceptor, and the operating conditions. Different electrode and separator materials vary in their physical and chemical properties (e.g., surface area, electric conductivity, and chemical stability), thus they also vary in their impacts on biofilm establishment, bacterial metabolism, ohmic resistance, and the rate of electrode reactions. Therefore, it is of interest to develop low-cost, high performance anode, cathode, and separator materials to promote the performance of MFCs.

3.1 Anode Materials

The anode is where the electroactive biofilm establishes and the bioelectrochemical reaction occurs. Therefore, anode materials play a significant role in MFC performance. An ideal anode would have high conductivity, high specific surface area or

porosity, low cost, biocompatibility, and good stability. Several metal materials, such as stainless steel, titanium, copper, nickel, and gold, and carbon materials, such as carbon cloth/paper, carbon graphite brush, and biomass-derived porous carbon, have been used for the anode of MFCs [6, 27–29]. Among these materials, the carbonaceous anodes are regarded as the most cost-effective and promising for the large-scale application of the MFCs.

3.1.1 Traditional Carbon Materials

Carbon materials (e.g., carbon cloth/paper, graphite plate/granules/rod, carbon mesh, carbon felt, reticulated vitreous carbon, and graphite brush) are widely used as anode materials because of their high conductivity and biocompatibility [6, 30–34]. Carbon cloth/paper is a planar, porous, but fragile and expensive, material so it is mainly used in lab-scale testing. Carbon felt and reticulated vitreous carbon are also porous materials and therefore can provide many inner spaces for bacteria growth and channels for substrate supply and proton removal. Unfortunately, the low electrical conductivity of carbon felt leads to high ohmic resistance, and the cost of reticulated vitreous carbon is too high for wastewater treatment use. Granular activated carbon (GAC) is also used as the anode because of its good biocompatibility and low cost [35]. Generally, GAC is usually used in packing-bed anodes, which produce low anode electrical conductivity. Additionally, the specific surface area of the GAC-based anode is quite high, but the surface area accessible to bacteria acclimation is relatively low because most of the pores in GAC are small pores with a diameter < 50 nm. The graphite brush electrode is one of the most promising anodes for practical application of MFC technology. The MFC using the graphite brush had a maximum power density of 2400 mW/m^2, which was about 4 times higher than using carbon paper (600 mW/m^2) [8]. A graphite brush is prepared by folding and twisting a titanium wire to form a succession of regular loophole openings in which graphite fiber bundles are crimped to form a spiral structure [36, 37]. The central titanium metal guarantees high electrical conductivity. The micro-scale diameter of graphite fibers ($\sim$7 μm) provides a highly open porous structure for bacterial acclimation. Graphite brushes have been extensively used as MFC anodes and ongoing investigations are focused on reducing the overall cost.

3.1.2 3D Porous Anode Base on Carbon Nanomaterials

To improve the anode performance, 3D materials with large surface areas are emerging as alternatives for the anode. A variety of 3D nanomaterial-based anodes, such as chitosan/vacuum-stripped graphene scaffold, 3D chitosan–carbon nanotube scaffolds, polyaniline hybridized 3D graphene, carbon nanotube (CNT)/polyaniline (PANI) nanocomposite, PANI/graphene-coated nickel foams, 3D carbon nanotube-textiles, porous carbon nanofiber aerogels, graphene-sponges, and

graphene-coated nickel foams have been studied as MFC anodes [19–26]. Katuri et al. fabricated a multiwall carbon nanotube (MWCNT)/chitosan 3D composite anode by ice segregation-induced self-assembly (ISISA). A maximum current density of 24.5 A/m^2 was achieved at 0 V versus Ag/AgCl for 200 h [38]. Chitosan/vacuum-stripped graphene scaffold and 3D chitosan–carbon nanotube scaffolds prepared using ISISA also exhibited a great advantage over carbon cloth or felt. Vacuum-stripped graphene powder randomly embedded on the chitosan layers increased the surface roughness of the layers and provided a larger graphene surface area for bacteria adhesion. In addition, due to the presence of meso/micropores in the anode, a large internal surface area was accessible to endogenous mediators for the electron transfer between bacteria and anode, leading to increased biofilm activity. An MFC using these anodes achieved 78 times higher power output than with the conventional carbon cloth [19]. These 3D porous nanomaterials-based anodes generally possess a hierarchical porous structure that benefits efficient diffusion of electron mediators and substrate as well as bacterial adhesion in the interior of the 3D electrode. They show great potential for use in MFCs.

3.1.3 Biomass Derived Materials

Many types of biomass, such as chestnut shells, pomelo peels, natural loofah sponges, and bamboo, have been used as precursors for the fabrication of the MFC anodes (Fig. 8) [39–42]. In general, the inherent pore structure of the biomass can evolve into macropores during carbonization at a temperature above 800 °C. The macropores are usually cross-linked, favoring a rather high conductivity and a high performance anode. For example, Chen et al. used sponge-like pomelo peels as the precursor for the anode. The MFC using the reticulated carbon foam derived from pomelo peels achieved a maximum current density of 4.0 mA/cm^2 [39], which was 2.5 times higher than that of graphite felt. Zhang et al. reported that carbonized dry bamboo branches can be directly used as the high performance anode for biofilm establishment because the obtained electrode maintained the inherent structure of bamboo, which is a hollow tube with an inner diameter of 2 mm and highly ordered 15–100-μm macropores [41]. A chestnut shell-derived porous carbon anode has also been tested. An MFC with this anode achieved a maximum power density (23.6 W/m^3) 2.3 times higher than carbon cloth anode (10.4 W/m^3) [42]. Anodes derived from corn stems, king mushrooms, and wild mushrooms have been reported by Karthikeyan et al. [43]. Lu et al. reported a high-performance flexible anode derived from carbonized silk cocoons. Due to their hierarchical 3D, pseudographitic microstructure, good biocompatibility, and high capacitance, an MFC equipped with the carbonized silk cocoon anodes provided ∼2.5-fold maximum power density greater than that of carbon cloth anodes [44]. The use of natural and recyclable materials can greatly reduce the cost of electrode materials and improve anode performance. These materials provide a potential avenue for MFC

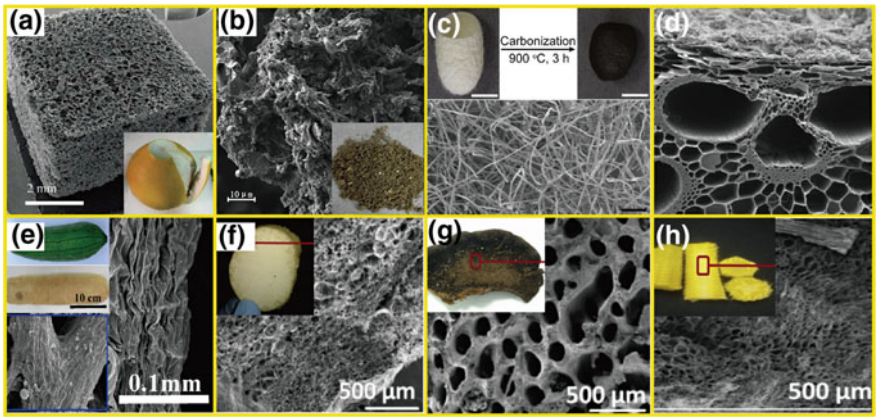

Fig. 8 3D porous anode materials derived from biomass: **a** pomelo peel (adapted and reprinted from [39], Copyright 2012, with permission from Royal Society of Chemistry), **b** chestnut shell (adapted and reprinted from [42], Copyright 2018, with permission from Elsevier), **c** silk cocoon (adapted and reprinted from [44], Copyright 2017, with permission from Elsevier), **d** bamboo (adapted and reprinted from [41], Copyright 2014, with permission from Elsevier), **e** natural loofah sponge (adapted and reprinted from [40], Copyright 2013, with permission from American Chemical Society), **f** king mushroom, **g** wild mushroom (adapted and reprinted from [43], Copyright 2015, with permission from Elsevier), and **h** corn stem (adapted and reprinted from [43], Copyright 2015, with permission from Elsevier)

commercialization. However, the structure of these materials is difficult to control and reproduce thus limiting their application in MFCs.

3.1.4 Modification of the Anode Materials

Modification of anode materials can improve MFC performance by increasing the bacterial affinity for the anode surface, by providing an extra supporting and conductive surface, or by facilitating the extracellular electron transfer (EET) between bacteria and the electrode. The modification methods can be classified into the following types: (1) decorating with carbon nanomaterials, (2) modification using a conducting polymer, and (3) chemical/electrochemical anode modifications.

The widely used nanomaterials for anode modifications are CNTs, carbon nanospheres, and graphene. CNTs are cylindrically-shaped carbon materials with a large surface area and these promote microbial adhesion and electron transfer between the bacteria and anode surface. Ren et al. reported that an anode with horizontally aligned spin-spray layer-by-layer CNT showed a smaller sheet resistance and induced a thicker biofilm than the unmodified samples. A maximum power density of 3320 ± 40 W m^{-3} was obtained by using the anode in a miniaturized MFC. This value was more than 8.5 times greater than values reported by prior-art MFCs using 2D and 3D nanostructured electrodes [45]. Similarly,

nitrogen-doped CNT not only facilitated EET from the c-cytochrome located on the outer membrane of the bacteria to the electrode but also enhanced the contact area between the bacteria and the electrode [46]. Graphene is a unique carbon nanomaterial with 2D lattice made of sp^2-hybridized carbon atoms. Graphene has great application potential in MFCs. Decorating the electrode with graphene can create an electrically conductive surface similar to that of CNT-coated materials while considerably reducing the electrode cost. A graphene-modified anode improved the power density and the energy conversion efficiency by 2.7 and 3 times, respectively [47]. Zhang et al. also demonstrated that the graphene-modified SSM anode produced a maximum power density of 2668 mW/m^2, which was 18 times larger than the unmodified SSM anode [48].

Conducting polymers, such as polyaniline and polypyrrole, have been widely used to modify the electrode due to their high conductivity and durability in MFC-relevant conditions. Polyaniline carries positive charges in neutral environments; therefore, it is attractive for enhancing the adhesion of the negatively charged bacteria. A polyaniline-coated anode reduced the start-up time of MFCs from 140 to 78 h by enhancing bacterial cell attachment [49]. The conducting polymer facilitated the EET between the bacteria and the anode. For example, a anode modified by polypyrrole/graphene oxide composites using electro-polymerization delivered an 8 times higher maximum power density than the unmodified anode in MFCs [50]. Gnana Kumar et al. reported that a reduced graphene oxide/polypyrrole composite-modified carbon cloth anode achieved a 3 times higher maximum power density than that of unmodified carbon cloth, due to the increased electron transfer efficiency and the increased contact area between the bacteria and the anode [51].

With chemical and electrochemical modifications, functional groups can be introduced onto the electrode surfaces, leading to a change in the physicochemical properties of the electrodes and creating a larger electrocatalytically active area, increased surface charges on the electrode, and a faster EET rate. Chemical and electrochemical modifications of the anode are effective methods for improving the anode performance due to the enhanced bacterial cell attachment and the facilitated EET rate from the bacteria to the anode surface. Chemical modification of the anode is usually carried out by directly soaking the electrode in strong acid or treating the carbon materials in ammonia at 600–800 °C [52–54]. Cheng et al. achieved a 48% increase in power production and a 50% decrease in the start-up time by treating the carbon cloth in ammonia at 700 °C [54]. However, chemical modification usually requires toxic chemicals and high temperatures, both of which increase the cost of MFCs. Anode modification can also be achieved by electrochemical oxidation in different electrolytes, such as NH_4NO_3, $(NH_4)_2SO_4$ and HNO_3/H_2SO_4 [55, 56]. Zhang et al. found that electrolyzing the carbon cloth in nitric acid followed by soaking in aqueous ammonia could produce a 58% higher maximum power density compared to the untreated control [55].

3.2 Separators

3.2.1 Ion Exchange Membrane

In the double-chamber MFCs (DCMFCs), the membrane is usually used to separate the anode and cathode chamber. This prevents the crossover of oxygen and substrate while allowing ion transfer between the anode and cathode chamber. The major types of membranes used in MFCs include cation exchange membranes (CEM), anion exchange membranes (AEM), and the polymer/composite membranes. Many CEMs, including Nafion, Hyflons, Zirfons, and Ultrexs CMI 7000, are used in DCMFCs. Nafions are the most commonly used CEM in MFCs because of their good proton conductivity resulting from the negatively charged hydrophilic sulfonate groups attached to the hydrophobic fluorocarbon backbone [57]. Usually, a thinner membrane has lower ohmic resistance and produces higher performance. For example, an MFC with a thinner Nafion 112 membrane had a higher power density of 31.32 mW/m^2 than one using a thicker Nafion 117 membrane (9.95 mW/m^2). Pant et al. investigated the effect of membrane types on MFC performance and found that an MFC with Ultrexs CMI 7000 had a comparable performance to that with the Nafion membrane [58], but had a lower oxygen mass transfer coefficient (2.8×10^{-4} cm/s) compared to one with Zirfons (1.9×10^{-3} cm/s) [59]. AEMs, such as AFN, AM-1, and ACS, are also widely used in MFCs. AFN had the lowest membrane resistance among these AEMs, resulting in the increased production of electricity [60]. However, AM-1 and ACS have a lower oxygen mass transfer coefficient compared with AFN. Polymer/composite membranes, such as sulfonated polyether ether ketone (SPEEK) membranes and disulfonated poly (arylene ether sulfone) (BPSH) membranes, are also used as alternatives to the Nafion membrane in MFCs. A high proton conductivity and a low oxygen mass transfer coefficient of the SPEEK membrane can be obtained by sulfonating the native PEEK membranes [61]. Leong et al. found that MFCs with a BPSH membrane had a higher performance than those with Nafion. This was due to the lower ohimic resistance and the lower extent of biofouling of the membrane resulting from the higher proton conductivity and the higher hydrophilicity of the BPSH membrane [60]. Although these ion exchange membranes can effectively prevent the crossover of oxygen and the substrate, their main problem is the pH imbalance created between the anode and cathode chambers. This is caused by the limited cation or anion transfer across the membranes, resulting in anode chamber acidification and cathode chamber alkalization [62, 63]. Anode chamber acidification and cathode alkalization leads to the inhibition of microbial activity, deterioration of the cathode catalyst activity, and a reduction in whole cell performance.

3.2.2 Other Porous Membranes or Separators

To overcome the ion exchange membrane problems, such as pH imbalance between the anode and cathode chambers, high costs, and high internal resistance, different porous membranes or separators have been proposed. Ultrafiltration membranes, microfiltration membranes, nylon and glass fiber filters, J-cloths, and polyether sulfone resin have been studied as separators for MFCs [64–67]. Fan et al. used J-cloth as the separator on the water-facing side of the air-cathode of an MFC. The CE was significantly improved from 35 to 71% due to the significant reduction of oxygen diffusion in the presence of the J-cloth [68]. Separators with a large pore size typically produce higher performance due to lower internal resistance. For example, Zhang et al. used nylon filters with different pore sizes as separators in MFCs. The power generation increased from 769 ± 65 to 941 ± 47 mW/m^2 when the pore size increased from 10 to 160 mm [67]. Porous membranes usually have a low internal resistance, compared to the ion exchange membranes, due to the porous structure. This structure benefits the ion transfer between the anode and the cathode. Therefore, the use of these porous membranes or separators can effectively prevent the diffusion of oxygen from the cathode to the anode, improve the CE, and alleviate the pH imbalance.

3.3 Cathode Materials

The design and fabrication of the cathode is a major challenge for MFC applications. To achieve high performance, aqueous cathodes using soluble electron acceptors with a high electrode potential (such as, potassium ferricyanide, and potassium peroxodisulfate) have been widely used [69, 70]. However, the electron acceptors must be replaced after depletion. This would create an additional cost for the treatment of wastewater and secondary pollution. Therefore, the air-cathode that uses oxygen as the electron acceptor is considered as the most promising cathode for practical applications due to the high electrode potential and the ready availability of oxygen. The main components of an air-cathode include ORR catalysts (to reduce the ORR overpotential), ionomer binders (to facilitate proton conduction in catalyst layers (CLs), and to tightly deposit the ORR catalysts), a hydrophobic layer (to permit air supply to the ORR catalysts and to prevent water leakage), and electrode supports (to provide mechanical support to CLs and to collect the electrons).

3.3.1 ORR Catalysts

In lab-scale MFCs, Pt is considered to be the most active catalyst for ORR. To achieve acceptable performance, the Pt loading of a typical MFC air-cathode needs to be ~0.5 mg cm^{-2} [71]. This would significantly increase the cost of

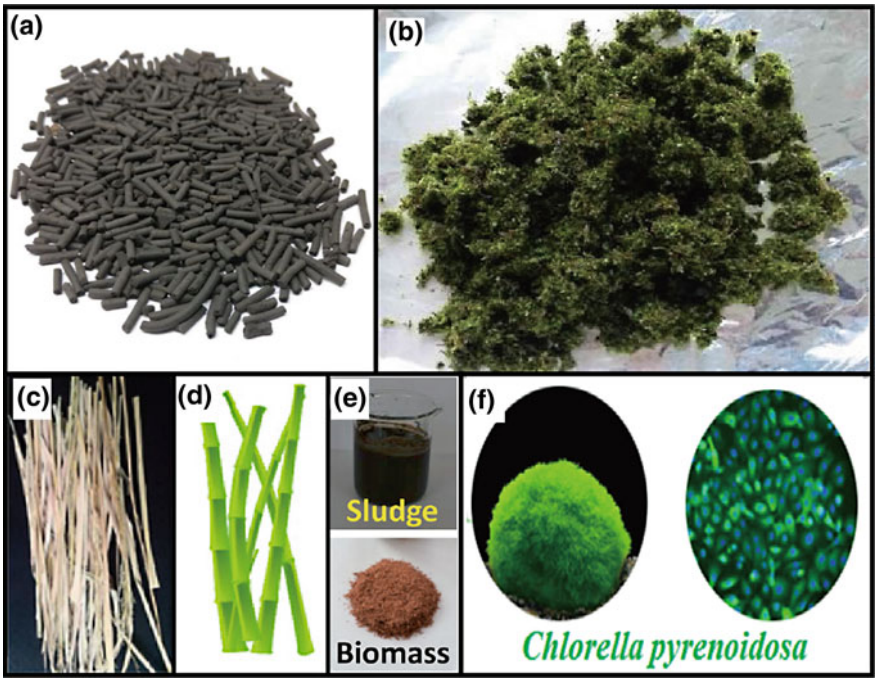

Fig. 9 Carbonaceous air-cathode catalysts derived from biomass: **a** activated carbon, **b** plant moss (adapted and reprinted from [75], Copyright 2016, with permission from Elsevier), **c** rice straw (adapted and reprinted from [76], Copyright 2015, with permission from Royal Society of Chemistry), **d** bamboo branches (adapted and reprinted from [73], Copyright 2017, with permission from Elsevier), **e** mixture of sludge and coconut shell derived powders (adapted and reprinted from [82], Copyright 2015, with permission from Royal Society of Chemistry), and **f** *Chlorella pyrenoidosa* (adapted and reprinted from [80], Copyright 2017, with permission from Elsevier)

commercial-scale MFCs. Carbon materials, such as activated carbon (AC) and biomass-derived carbons, exhibit comparable or higher ORR activity compared to Pt [72, 73]. Watson et al. reported that an air-cathode using the coal-derived AC catalyst had a higher performance than Pt/C. Watson et al. also compared the ORR activity of the catalysts with those derived from peat, coconut shell, hardwood, and phenolic resin, and found that the ORR activity of the catalysts was dependent on the precursors [74]. Since then, various types of plant biomass (plant moss, rice straw, bamboo, sludge, and microalgae) (Fig. 9), have been proposed as precursors for the carbonaceous ORR catalysts [73, 75, 76]. Sun et al. prepared a cornstalk-derived nitrogen-doped carbonaceous catalyst to facilitate ORR and obtained a maximum power density of 1122 ± 32 mW/m^2 in MFCs [77]. Zhou et al. synthesized a self-assembled carbon nanoparticle-coated porous ORR catalyst from plant moss and achieved a maximum power density of 703 ± 16 mW/m^2 (Fig. 9b) [75]. In addition to plant biomass, animal biomass, such as eggs, blood,

bones, urea, and animal liver, have also been used as precursors for ORR catalysts. Wang et al. synthesized non-precious tremella-like mesoporous carbon as the ORR catalyst using carbonized egg white as the carbon source [78]. Wu et al. developed an ORR catalyst based on co-doped mesoporous carbon microspheres from the ecofriendly biomass of eggs without the introduction of extrinsic dopants [79]. Microalgae, such as *Chlorella* spp., with a high nitrogen content between 4–8% have been proposed as the precursor for a cost-efficient ORR catalyst in MFCs. The catalyst derived from *Chlorella pyrenoidosa* can achieve a higher power generation (>2000 mW/m^2) than with Pt/C (Fig. 9f) [80]. Sludge that is usually regarded as an unwanted byproduct of wastewater treatment was also used as the precursor for the ORR catalyst due to high N and metal levels. Deng et al. found that N, P, and Fe heteroatom-doped hierarchical carbon catalysts with honeycomb-like interconnected macro-mesoporous frameworks can be obtained by direct pyrolysis of livestock sewage sludge. A maximum power density of 1273 ± 3 mW/m^2 can be obtained when this catalyst is applied in MFCs, and this power density is comparable to that of commercial Pt/C (1294 ± 2 mW/m^2) [81].

3.3.2 Binders

Nafion is commonly used as the binder for the ORR catalyst due to its high proton conductivity. Nevertheless, the high cost of Nafion restricts large-scale use. Several less expensive polymers, such as polytetrafluoroethylene (PTFE), polydimethylsiloxane (PDMS) and polyvinylidene fluoride (PVDF), could be alternatives to Nafion. For example, Dong et al. reported that the air-cathode using AC as the ORR catalyst and PTFE as the binder showed a higher performance than that using Nafion because of the improved oxygen supply [83]. The CL preparation process using PTFE as the binder can have a significant impact on MFC performance. A 35% higher performance was obtained by avoiding sintering during CL preparation compared to the use of sintering because sintering reduced the pore area and the porosity of CL and led to a deteriorated oxygen supply to the CL [84]. Yang et al. proposed an easy way to manufacture inexpensive air-cathodes using PVDF as the binder. The PVDF-based cathode was feasible in MFC operation because a cheap, but high-performance MFCs can be achieved [85]. The binder content in the air-cathode has an optimum value. High binder loading can increase the ohmic resistance of the electrode because binders are usually an electrical insulator, while a low binder loading can lead to the detachment of catalyst powder from the catalyst layer [86]. In addition, the binders are usually hydrophobic and can obstruct H^+ and OH^- supply towards the CL, contributing to an additional cathodic potential loss of the air-cathode in MFCs [87, 88].

3.3.3 Electrode Supports

Carbon cloth/paper (Fig. 10a) is widely used in both anode and air-cathode fabrication. The common electrode supports for the cathode are carbon cloth/paper and graphite paper, on which the catalyst ink is coated on the water-facing side and the waterproofed layer is applied on the air-facing side [89]. However, the friability and the high cost of carbon cloth/paper and graphite paper hampers large-scale application for wastewater treatment. Recently, nickel foam, nickel mesh, and stainless steel mesh (Fig. 10b–d) have been reported as alternatives to carbon cloth/paper due to their high electrical conductivity and their high stability in MFC-relevant conditions. Zhang et al. proposed a method to prepare air-cathodes by pressing CL onto nickel mesh, which was used as a cathode support and current collector, avoiding the need for carbon cloth and reducing the cost [72]. Cheng and Wu studied the use of nickel foam as the current collector in air-cathode preparation. Their results indicated that the nickel foam cathode could be used in scaling up the MFC system [86]. With high corrosion resistance and electrical conductivity, metallic nickel remains a metal material that is too expensive for large-scale applications. To reduce the cost of cathode fabrication, Dong et al. reported SSM as

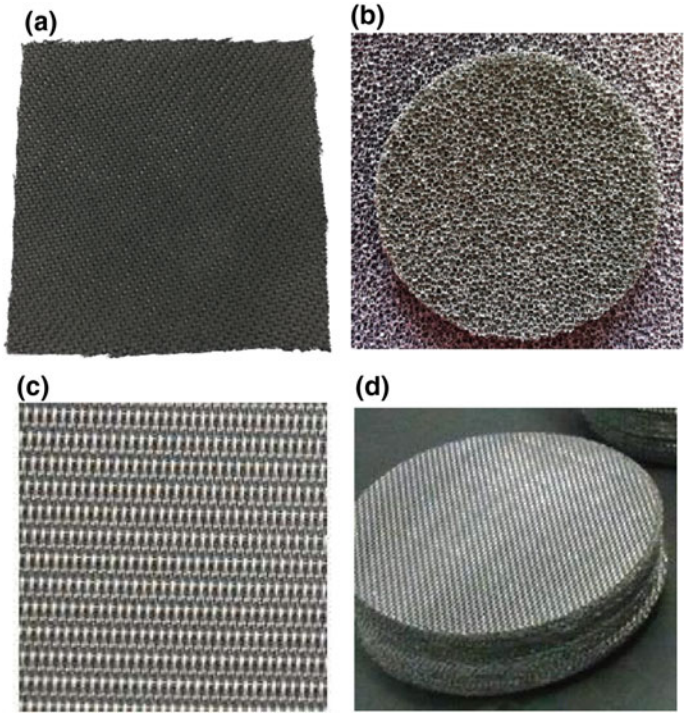

Fig. 10 Air-cathode supports or current collector in MFCs: **a** carbon cloth, **b** nickel foam, **c** nickel mesh, and **d** stainless steel mesh

an alternative to nickel foam and mesh in the cathode [6]. Usually, SSM is corrosion resistant, with high electrical conductivity, and low cost, being overall superior to nickel mesh/foam. The SSM can be directly used as a cathode support and current collector by pressing CL and a gas diffusion layer (GDL) on its two sides, respectively. Li et al. optimized the opening size of SSM in an AC air-cathode and reported that a cathode using SSM with 40 M had a better performance due to the lower internal resistance [90]. So far, SSM remains one of the most widely used cathode supports for the air-cathode of MFCs.

4 MFC Architecture

4.1 Double- and Single-Chamber MFCs

Various MFC architecture has been reported and the majority of it fall into the categories of cubic, cylindrical, H-cell, and plate- and tube-shaped reactors. Based on different working principles, the MFC can be categorized into paper-based MFCs, microfluidic MFCs, plant MFCs, and sediment MFCs. Although there are many kinds of MFC designs intended for scale-up and practical application, MFCs can be classified into DCMFCs and single-chamber MFCs (SCMFCs) depending on whether an ion exchange membrane is used. The advantages of SCMFCs are reduced setup costs due to the absence of an ion exchange membrane and the direct usage of freely available oxygen in the air as electron acceptors. The drawbacks of SCMFCs are the decreased CE that results from oxygen crossover from the cathode to the anode and a low power density caused by the thermodynamic and kinetic constraints of ORR in the cathode. The ion exchange membrane in DCMFCs reduces oxygen crossover to the anode and, thus, leads to enhanced CE of the MFCs. However, the pH imbalance between the anode and cathode chamber, which is caused by the limited proton transfer across the proton exchange membrane, results in anode chamber acidification, which leads to the inhibition of microbial activity and reduced performance.

4.1.1 DCMFCs

DCMFCs are composed of anode and cathode chambers separated by an ion exchange membrane, which prevents the mixing of anolytes and catholytes (as described in Sect. 3.2). This feature allows the use of an immersed cathode in MFC. For example, Zhang et al. developed a plate-shaped DCMFC using potassium ferricyanide as the cathode electron acceptor (Fig. 11b) [70]. Many immersed cathodes using soluble electron acceptors with high redox potentials, such as persulfate, permanganate, triiodide, and hydrogen peroxide, have been proposed for

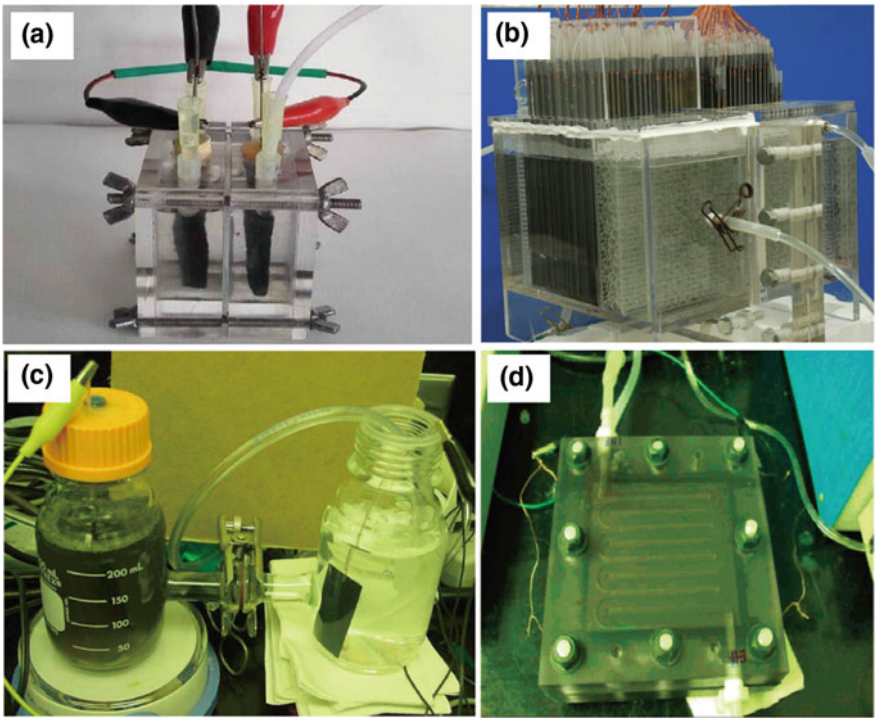

Fig. 11 Pictures of DCMFCs: **a** cubic MFC (adapted and reprinted from [94], Copyright 2015, with permission from Royal Society of Chemistry), **b** liter-scale MFC (adapted and reprinted from [32], Copyright 2013, with permission from Elsevier), **c** bottle-based H-shape MFC (adapted and reprinted from [95], Copyright 2005, with permission from Elsevier), and **d** plate MFC (adapted and reprinted from [96], Copyright 2004, with permission from American Chemical Society)

the DCMFC cathode [69, 91–93]. However, these electron acceptors are not regenerative in ambient conditions and need to be replaced after they are depleted.

The use of membranes in DCMFCs can also limit the oxygen diffusion from cathode to anode. A significant increase in CE occurs compared to SCMFCs since the membrane suppresses the oxygen crossover from the cathode to the anode chamber and thus decreases the aerobic substrate degradation. Existence of an ion exchange membrane allows for very small electrode spacing, and can significantly reduce the ohmic resistance of the MFC and improve MFC performance. Zhang et al. designed a plate MFC in which the anode and cathode were pressed onto the two sides of a cation exchange membrane, respectively (Fig. 11d) [70]. However, other cation species in the anolytes usually have a significantly higher concentration than protons, making the flux of proton transport considerably lower compared to the transport of other cations. This causes acidification of the anode chamber and decreased anode performance.

4.1.2 SCMFCs

SCMFCs eliminate the membrane between the anode and the cathode and enable a simple design and a lower fabrication cost. A SCMFC only contains a single chamber coupled with a porous air-cathode exposed to the atmosphere. This eliminates the requirement of aeration in the cathode chamber. In a SCMF, protons are transferred from the anode to the porous air-cathode through the electrolyte by diffusion. Liu et al. reported the first SCMFC consisting of an anode placed inside a plastic cylindrical chamber and a cathode assembled outside (Fig. 12a) [97]. Cheng et al. designed a single-chamber MFC with a cylindrical structure. The air-cathode made of carbon cloth and Pt/C was wrapped around the cylindrical reactor [98]. The proton transfer resistance in SCMFCs is much lower than that of DCMFCs due to the absence of the ion exchange membrane. However, compared to DCMFCs, the oxygen diffusion from the cathode to the anode is higher in SCMFCs, leading to a larger amount of aerobic degradation of the substrate. A considerable amount of substrate is consumed by bacterial growth on the anode, rather than electricity generation, and this leads to a lower CE. For example, Liu et al. reported that a DCMFC can achieve a CE value of 40–55%, while a CE value of only 9–12% is possible for a SCMFC [97].

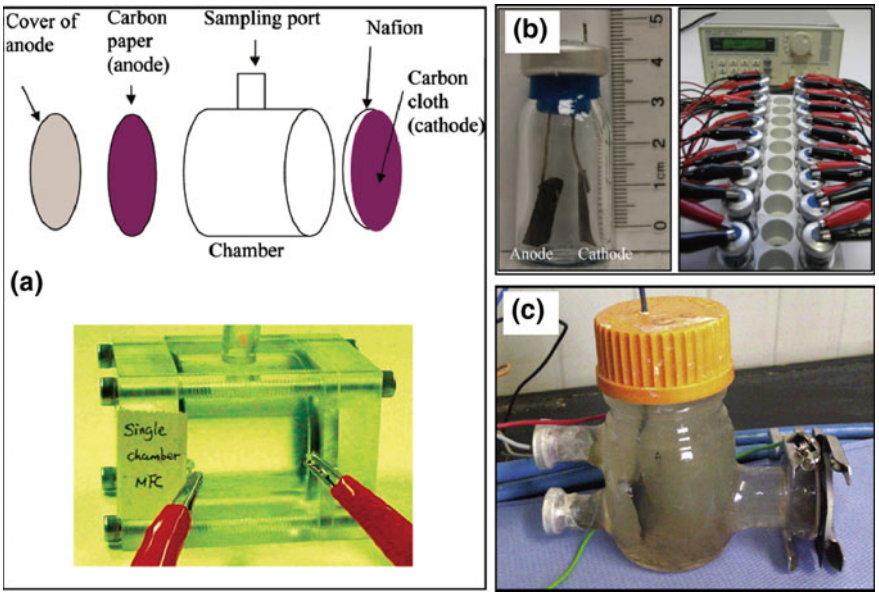

Fig. 12 Single-chamber MFCs: **a** structure of a cubic single-chamber MFC (adapted and reprinted from [97], Copyright 2004, with permission from American Chemical Society), **b** bottle-based single-chamber MFC (adapted and reprinted from [99], Copyright 2011, with permission from Elsevier) and **c** bottle-based single-chamber MFC (adapted and reprinted from [100], Copyright 2013, with permission from Elsevier)

4.2 Air-Cathode MFCs

4.2.1 Designs of Air-Cathode MFCs

Air-cathode MFCs are considered to be promising architecture for scaling-up because the cathode is directly exposed to the air and it does not require additional energy to supply oxygen. The air-cathode can be integrated in flat plate, cubic, and tubular MFCs. Air-cathode MFCs with plate and cubic architecture typically consist of rectangular anode chambers, and the air-cathode is assembled on the side opposite the anode. Compared with the cubic design, the flat plate MFC has a lower ohmic resistance because the design minimizes the spacing between the anode and the cathode [101]. Tubular structures are also widely used to design air-cathode MFCs. The tubular MFC is typically composed of an anode surrounded by a porous separator and the cathode is wrapped outside the separator. The separator is used to avoid an electrical short-circuit between the anode and cathode and to maximize the CE. Perforated cylindrical materials, such as polyvinyl chloride or polypropylene tubes, are usually used as the mechanical support [102, 103]. The tubular architecture is optimal for scaling-up, since it enables sufficient substrate supply, product removal, and continuous operation [104]. During scale-up, this architecture could be enlarged by simply extending the tube in the axial direction. In addition, when it is operated in continuous-feed mode, tubular MFCs only need a simple manifold to distribute water into various reactors.

4.2.2 Air-Cathode Fabrication

To achieve acceptable cathode performance, a good air-cathode should provide a large amount of triple-phase boundaries (TPB) with oxygen, protons, and electrons simultaneously present. In order to provide sufficient TPBs, the air-cathode usually consists of several layers, including the CL, the hydrophobic layer, the GDL, and the carbon paper/cloth support. The fabrication method for the air-cathode has a great influence on the physical and chemical properties of these layers, and therefore greatly affects the performance of the air-cathode. The approaches used to prepare the air-cathode of MFCs can be classified as follows:

Carbon Cloth/Paper Based Cathode Using Spray/Brushing Methods

Spray/brushing is a common method for the fabrication of air-cathodes. It usually involves sequentially preparing the hydrophobic layer or GDL on the air-facing side of the carbon material support and the CL on the water-facing side of the carbon material support. The hydrophobic layer, or GDL, is made by spraying 15–60 wt% PTFE suspension onto the carbon material supports to facilitate the air supply and to prevent water leakage from the reactor [71]. Cheng et al. prepared an air-cathode

by brushing the Pt catalyst and a mixture of carbon black and 30% wt. PTFE solution onto water-facing and air-facing sides of the carbon cloth serving as the CL and the hydrophobic layer, respectively. Cheng el al. studied the effects of the number of hydrophobic layers on the performance of the air-cathode. An increase in the cathode potential of 117 mV and a CE increase of 171% were achieved with four hydrophobic layers, respectively [105]. A sintering temperature, ranging from 340 to 370 °C, is needed during the cathode fabrication process to achieve a uniform PTFE distribution. This causes significant changes in the physicochemical properties of the ORR catalysts and in the pore structures of the GDL and CL. Therefore, other fluoropolymers, such as PVDF with low melting points (melting point 177 °C), have been used to form the hydrophobic layer. Qiu et al. used PVDF to prepare the hydrophobic layer of the air-cathode and showed that the PVDF based air-cathode outperformed the PTFE air-cathode [106]. To minimize the ohmic resistance between the CL and carbon material supports, GDLs are usually added between the CL and carbon material supports by directly spraying the mixture of carbon black and PTFE suspension onto the carbon material supports. Santoro et al. found that the presence of the GDL substantially reduced the water loss and biofilm infiltration into the CL, thus enhancing the MFC performance [107].

Cold- and Rolling-Press Method

To meet the requirements of a large cathode size and ease of fabrication for commercialization, Zhang et al. proposed the cold press method for cathode fabrication [72]. In this method, a mixture of catalyst/PTFE and carbon black/PTFE was pasted on both sides of a nickel mesh current collector and cold-pressed at a pressure of 150 bar. Dong et al. proposed a rolling-press method for preparing the MFC air-cathode using SSM as the current collector. In this method, the CL and GDL were first prepared by rolling-press and then they were rolled onto the SSM. The rolling-press method is an accurate, labor-saving fabrication process and it can produce an air-cathode with high ORR activity [6]. SSM properties, such as opening size and density, can have a great influence on cathode performance because they affect the oxygen transfer, ion transfer, and electrical conductivity of the cathode [90]. Besides the properties of the SSM, the pressing conditions also influence the cathode performance because the porosity and electrical conductivity of the CL is closely related to the pressing pressure and temperature. For example, Zhang et al. found that the CL prepared under a lower pressure induced a higher total pore volume of the GDL and the CL and thus resulted in higher performance [108]. In order to increase the pore volume of the GDL and CL, the addition of a pore former is also a feasible way for increasing MFC performance. Liu et al. attempted to increase the porosity of the air-cathode by mixing the ACs with pore formers (NH_4HCO_3). They found that the improved porosity induced by the pore formers produced a higher exchange current density of ORR due to the extended TPBs [109]. Another factor affecting cathode performance is catalyst loading.

Yang et al. found that increasing the AC catalyst loading at levels of up to 27 mg/cm^2 improved the performance of the air-cathode due to the increased ORR active sites. However, a further increase in the catalyst loading from 27 to 62 mg/cm^2 only had a minor impact on cathode performance [110]. This was because the beneficial effects of increasing the catalyst loading were overwhelmed by the increased electrical resistance and oxygen diffusion resistance of the CL, resulting from the increased catalyst loading.

Self-assembly or Self-Standing Electrode

Many efforts have been made to optimize air-cathode fabrication. The process is complex, since it usually involves the preparation of CL and GDL, as well as their assembly on the current collector or electrode support. Therefore, the development of an easy fabrication method for the air-cathode is important for the practical application of MFCs. Several reports have presented methods for fabricating the self-assembly or free-standing cathode for ORR. Yang et al. reported a 3D nitrogen-enriched iron-coordinated CNT sponge cathode by two-stage chemical vapor deposition (Fig. 13a) [111]. The MFC with the prepared cathode delivered a higher power density (20.3 W/m^3) than that of the Pt/C cathode (12.8 W/m^3). Wu et al. developed 3D nitrogen-doped graphene aerogel-supported Fe_3O_4 nanoparticles for ORR through hydrothermal self-assembly and freeze-dry fabrication processes [112]. Although the price of graphene and CNT is still too expensive for using MFCs in wastewater treatment, the approaches provide new ways to prepare the self-assembly or free-standing electrode with low-cost carbon or biomass. Yang et al. proposed that heat-treated bamboo charcoal tubes (BCT), fabricated by directly carbonizing bamboo tubes, can be used as the monolithic air-cathode of MFCs [66]. In the BCT cathode, the carbonized N- and P-doped carbon can be directly used to catalyze the ORR without the involvement of PTFE and/or Nafion binder for CL fabrication. In the air-cathode, the inherent porous and tubular structure derived from BCT (Fig. 13b) can serve as oxygen or proton transfer channels, and the monolithic structure support, respectively. The MFC using the BCT cathode showed a power output (40 W/m^3) that was similar to the MFC using Pt/C.

5 Stacked MFCs

5.1 Power Generation of MFC Stacks

The power density of MFCs has increased several orders of magnitude over initial designs due to the optimization of reactor configuration, improvement of operational parameters, use of bacteria with greater electrochemical activity, and the

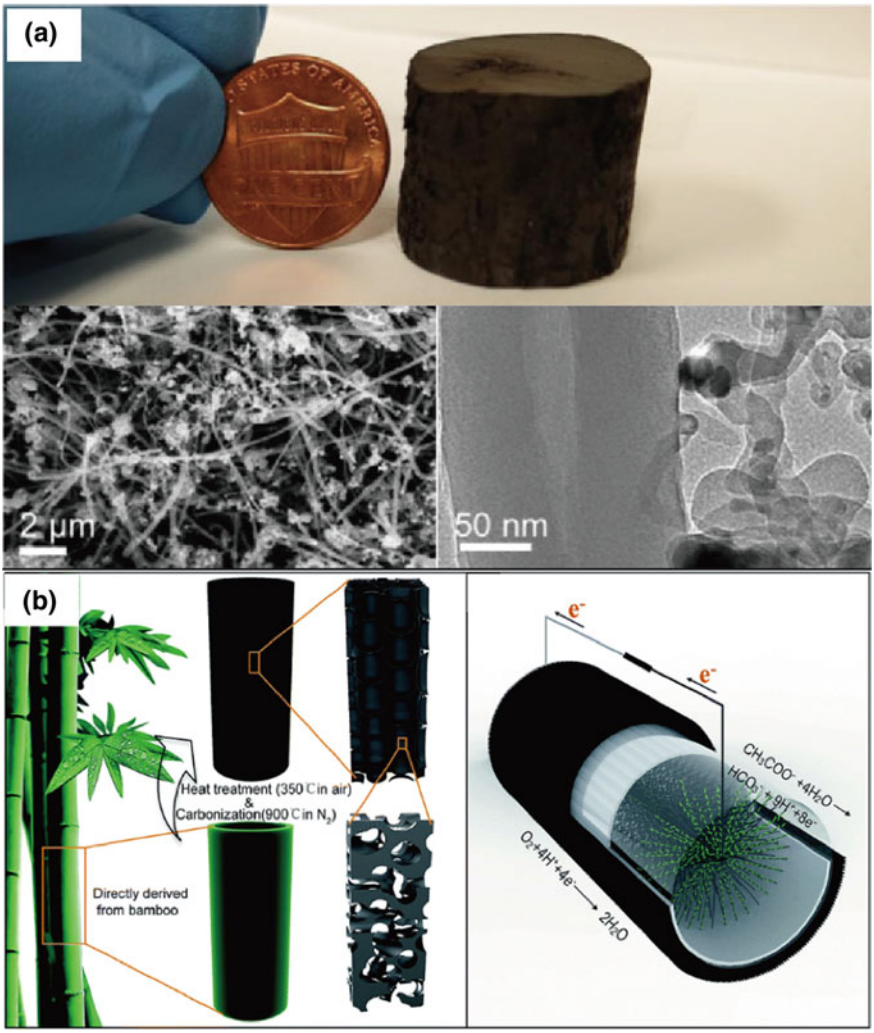

Fig. 13 Monolithic or free-standing cathode used in MFCs. **a** CNT sponge as a self-standing cathode (adapted and reprinted from [111], Copyright 2016, with permission from Elsevier), **b** bamboo charcoal tube derived air-cathode (adapted and reprinted from [66], Copyright 2017, with permission from Royal Society of Chemistry)

application of novel electrode materials. However, the practical application of MFCs remains limited by low voltage output. For example, the theoretical voltage output of MFC is $\sim$1.1 V when oxygen and sodium acetate are used as the electron acceptor and the electron donor, respectively, but the practical operating voltage is only $\sim$0.5 V. This is much lower than the theoretical value due to the charge transfer, ohmic, and mass transport overpotentials. In addition, the power density of

MFC is decreased with the increase of MFC volume, and it is very difficult to improve the power output by directly scaling up the MFC size. Therefore, stacking multiple MFCs in parallel or series is a promising strategy to realize the enhanced power and current output in practical application.

MFC stacks connected in parallel results in a current equal to the sum of the individual MFCs, while keeping a voltage equal to the average of the individual MFCs. For example, Wu et al. reported that an MFC stack constructed with five MFC units achieved a power density of 50.9 ± 1.7 W/m^3, which was about five times higher than that of the individual MFCs (~ 10 W/m^3) [113]. Aelterman et al. suggested that six individual continuous MFC units in a stacked configuration produced a maximum power output of 258 W/m^3, which was approximately six times higher than that of the individual MFCs [114]. In contrast to MFC stacking in a parallel connection, connecting multiple individual MFCs in series is an efficient way of achieving a high-voltage output. Theoretically, the voltage output from a series stack of MFCs should be the sum of the voltage outputs of the individual MFCs. For example, Gurung et al. showed that two MFCs stacked together in series could produce an OCV that equaled the mathematical sum of the individual MFCs [115].

Attempts have been made to build different MFC stacks using approaches, such as scaling-up by miniaturization and multiplication. Many types of MFC stacks, such as tubular, multi-electrode, cassette-electrode, and baffled MFC stacks, have been proposed to improve electricity generation or wastewater treatment (Fig. 14).

5.2 Limitations of Stacked MFCs

Although MFC stacks have shown to be an efficient approach to enhance the voltage and current output of MFCs, voltage reversal could cause system failure or a significant reduction of power generation in an MFC stack. Voltage reversal, which has usually been observed in series-connected MFC stacks, is a phenomenon where the voltage of an individual MFC in an MFC stack reverses from a positive to a negative value [123]. Voltage reversal in stacked MFCs is the result of non-spontaneous anode/cathode overpotential in a unit MFC that has sluggish anode/cathode kinetics compared to the other unit MFCs. For example, Oh et al. demonstrated that fuel starvation in an active cell, or a lack of power generation in the absence of bacterial activity in a unit cell (abiotic conditions) induced voltage reversal, due to the insufficient voltage of a unit cell compared to other cells [123]. An et al. also showed that the sluggish reaction rate of the anode in the weak MFC was responsible for voltage reversal in an MFC stack [124]. Voltage reversal in stacked MFCs can also be caused by slow cathode kinetics. For example, An et al. demonstrated that the inefficient catalytic activity of the ORR catalyst was the main reason for the voltage reversal in the stacked MFCs. They also showed that the voltage reversal can shift from the cathode to the anode when the anode performance became the limiting factor of the unit MFC [125]. Therefore, voltage

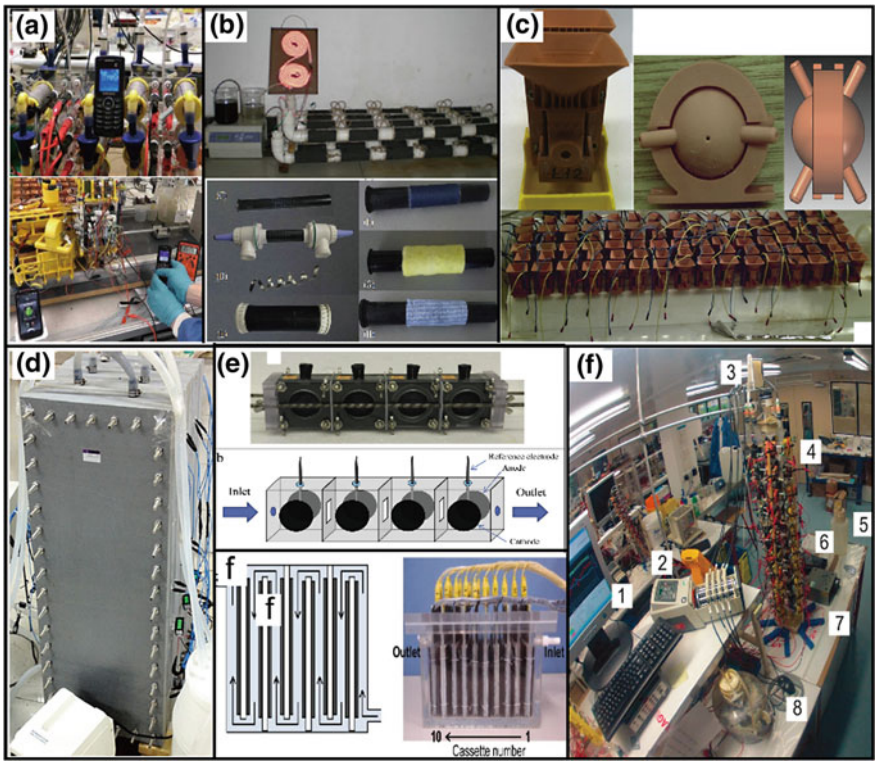

Fig. 14 Different MFC stacks using for power generation and wastewater treatment. **a** MFC stacks using for powering mobile phone (adapted and reprinted from [116], Copyright 2013, with permission from Royal Society of Chemistry), **b** tubular MFC stack (adapted and reprinted from [117, 118], Copyright 2012, Copyright 2016, with permission from Elsevier), **c** MFC stacks for urine utilization (adapted and reprinted from [119], Copyright 2013, with permission from Elsevier), **d** pilot-scale MFC stack (adapted and reprinted from [113], Copyright 2016, with permission from Elsevier), **e** multi-electrode MFC stack (adapted and reprinted from [120], Copyright 2014, with permission from Elsevier), **f** cassette-electrode MFC stack (adapted and reprinted from [121], Copyright 2013, with permission from Elsevier), (g) self-sustainable MFC stack (adapted and reprinted from [122], Copyright 2013, with permission from Royal Society of Chemistry)

reversal is a dynamic phenomenon that occurs in response to the dominant kinetic bottlenecks in the electrode or unit.

To avoid the requirement of a complicated water distribution system to pump substrate individually to different reactors and discharge separately, the MFC stack can be operated under a continuous-flow mode, in which the MFC units are hydraulically connected by substrate flow. However, as the MFC stack was operated with both electrical and hydraulic connections, substrate cross-conduction is usually observed because of the parasitic current flow in the parasitic fuel cell. This results in reduced performance during the MFC operation (Fig. 15). Zhuang and

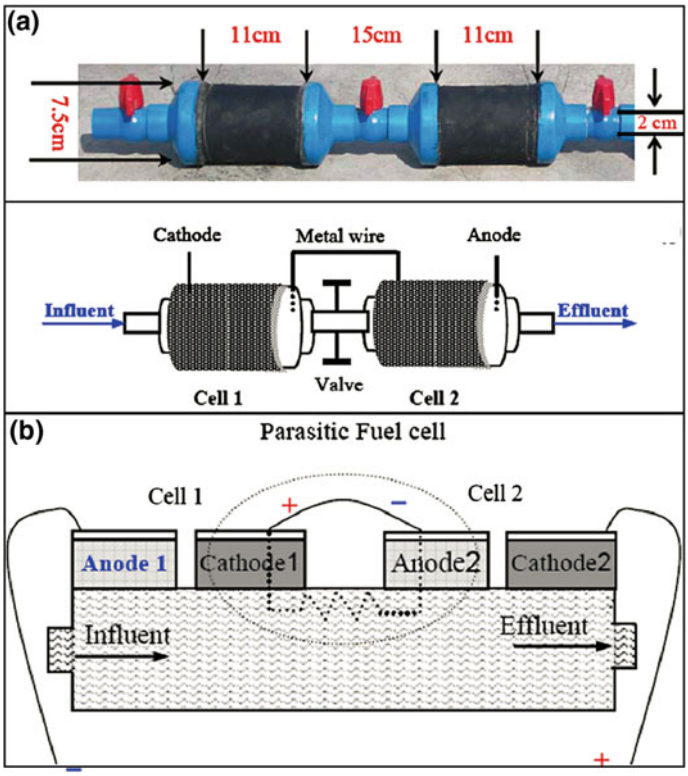

Fig. 15 Illustration of substrate cross-conduction effect between the serially connected MFCs (adapted and reprinted from [104], Copyright 2009, with permission from Elsevier)

Zhou suggested that two hydraulically connected MFCs could result in a 200–300 mV open-circuit voltage loss compared to the electrically isolated MFCs [104].

5.3 Maximizing Power Generation

Voltage reversal is a key factor limiting the power output in electrical series-connected MFCs, and attempts have been made to reduce this problem. One effective method is to keep the current density of the unit MFCs below the critical current density using an additional electrical circuit or device during the power generation (Fig. 16). For example, Wu et al. adopted a DC/DC booster circuit to convert the low DC voltage of the MFCs (0.2–0.4 V) to a more practical electronics range of >3.0 V, instead of stacking MFCs in a series [126]. A maximum power point tracking algorithm proposed by Boghani et al. was used to set the operating point of the MFC to optimize power harvesting [127]. An et al. used a threshold

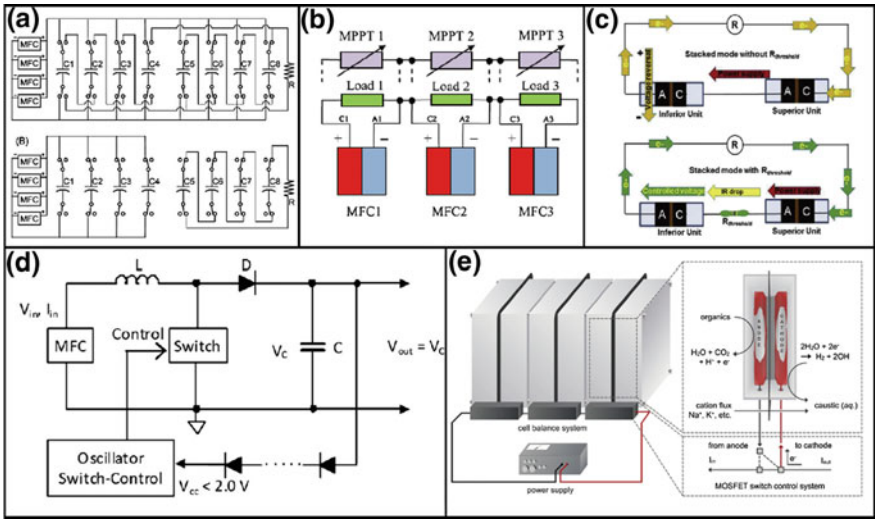

Fig. 16 Different methods to avoid or alleviate voltage reversal in MFC stacks. **a** An electronic circuit containing two sets of multiple capacitors that were alternately charged and discharged (adapted and reprinted from [129], Copyright 2011, with permission from Royal Society of Chemistry), **b** MFC subsystem series connectivity along with maximum power point tracking (adapted and reprinted from [127], Copyright 2014, with permission from Elsevier), **c** a threshold resistance for MFC stack (adapted and reprinted from [128], Copyright 2015, with permission from Elsevier), **d** a low power DC/DC booster circuit (adapted and reprinted from [126], Copyright 2012, with permission from Elsevier), **e** assistance current or voltage for MFC stack (adapted and reprinted from [132], Copyright 2013, with permission from Royal Society of Chemistry)

resistance to limit the operating current density of an MFC stack to a lower level than the critical current density and thus prevent voltage reversal in the MFC stack [128]. However, these methods are usually energy-consuming. To maximize energy harvesting, Kim et al. used an electronic circuit containing two sets of multiple capacitors that were alternately charged in parallel and discharged in series to increase continuous power production [129]. This electronic circuit boosted the voltage of the MFC stack and can be used to power an a microbial electrolysis cell (MEC) without the risk of voltage reversal. Compensating the non-uniformities in power output between the individual MFCs using electronic circuits was also used to prevent voltage reversal. For example, Khaled et al. demonstrated that the cell voltage of MFCs in a stack can be equalized using this balancing method [130]. Similarly, Yang et al. proposed a series-parallel-connected hybrid MFC stack and demonstrated that this connection can promote both the voltage, the current output, and the stable operating time of the stack in comparison to the series and parallel connected stacks by alleviating voltage reversal [131].

In addition, an efficient approach is the application of an external assistance potential or current on the individual MFCs to balance the inequalities and alleviate

the risk of voltage reversal. Andersen et al. reported a cell balance system that controlled the unit cells connected electrically in a series to maintain the cell voltage of individual cells at, or below, a maximum set point to prevent voltage reversal [132]. Kim et al. proposed an assistance-current method to prevent voltage reversal by connecting a supporting electrode in parallel and adjusting the assistance current flowing from the supporting electrode [133].

6 MFC Technologies and Applications

6.1 Wastewater Treatment

MFCs were first proposed for wastewater treatment in 1991. MFCs have tremendous substrate (fuel) versatility [7–9]. They can be operated using various readily bioconvertible organics ranging from pure compounds to complex mixtures in wastewater, such as acetate, glucose, and lactate. Acetate is commonly used as a substrate because of its inertness towards alternative microbial conversion (fermentations and methanogenesis) at room temperatures. Compared to acetate, glucose, lactate, or mixed organic pollutant-fed MFCs have a lower CE value due to the electron loss by competing bacteria. Domestic wastewater, such as brewery, starch processing, dye wastewater, and even landfill leachates, have also been used as substrates in MFCs for simultaneous electricity generation and wastewater treatment [10, 11, 13–16]. Processes that can generate electricity during different wastewater treatments will help to reduce the economic burden of wastewater treatment and provide a green alternative for electricity generation.

6.2 MFC Coupled System

MFCs are usually used as the on-site electrical power source for other microbial energy conversion systems to minimize the use of electricity from the local electrical grid. Wang et al. coupled MFCs with MECs to form an MFC-MEC system to convert the energy contained in wastewater into hydrogen [134]. In the system (Fig. 17a), the electricity produced by MFCs (at ~0.5 V) was used to power MECs (0.110 V in theory, >0.2 V in practice). Therefore, the integration of MFCs and MECs can reduce the need for additional electrical grid energy. Sun et al. combined a single two-chamber MEC (450 mL) with an MFC (225 mL) and achieved a maximum hydrogen production rate of 0.0149 m^3 H_2/day [135].

Besides their use for powering MECs, MFCs can also be combined with bioreactors for continuous effluent treatment to achieve maximum substrate utilization [136, 137]. Many soluble fermentation byproducts, such as formate, lactate, propionate, acetate, and butyrate, can be degraded in MFCs. Li et al. investigated

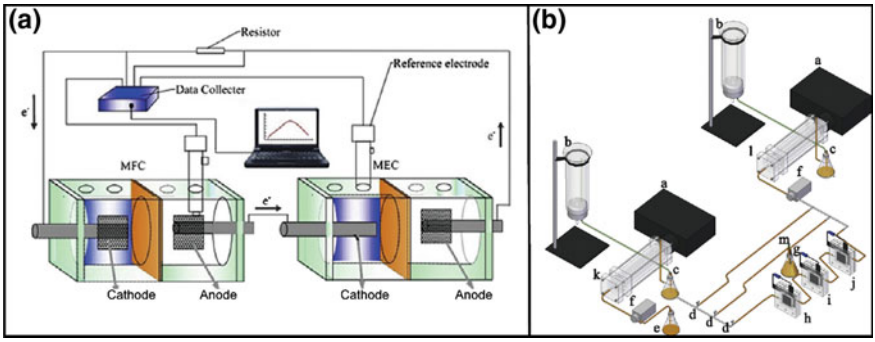

Fig. 17 Common used MFC coupled system. **a** MFC-MEC coupled system (adapted and reprinted from [139], Copyright 2014, with permission from Elsevier), **b** MFC-PBR coupled system (adapted and reprinted from [138], Copyright 2013, with permission from Elsevier)

the feasibility of using MFCs for pH adjustment and inhibitory byproduct removal for photobiohydrogen reactors (PBRs). In this study (Fig. 17b), single-chamber MFCs were connected between two series-connected PBRs. The coupled system achieved a significantly higher hydrogen production rate and substrate utilization due to the beneficial role of MFCs for pH adjustment and inhibitory byproduct removal [138].

6.3 Biosensors

MFCs can be used as biosensors for pollutant analysis and in situ process monitoring. In an MFC-based sensor, the chemical signals are usually the current or electrode potential generated from the substrate oxidation by the electroactive bacteria in the anode. The signals are directly related to factors, such as pH, substrate concentration, and toxin concentration (Fig. 18), and thus can be used to monitor the water quality [140]. The design of the MFC type of biosensor integrates the advantages of the whole-cell biosensor and the self-powered MFC device. This unique design provides featured compact sensor configuration, in which the microorganisms directly generate readable electric signal output without any externally powered transducer. Different types of MFCs have been used as biosensors for different purposes. Compared with other types of MFCs, the SCMFC type of biosensors are the most promising because aeration, recycling, and chemical regeneration of the catholyte is not required during the operation. For example, Lorenzo et al. constructed a biosensor based on the working principles of SCMFCs and demonstrated that the biosensor can be used as a probe for labile organics [141]. According to the application purposes, the MFCs can be designed as biosensors for monitoring biochemical oxygen demand/COD, toxic component

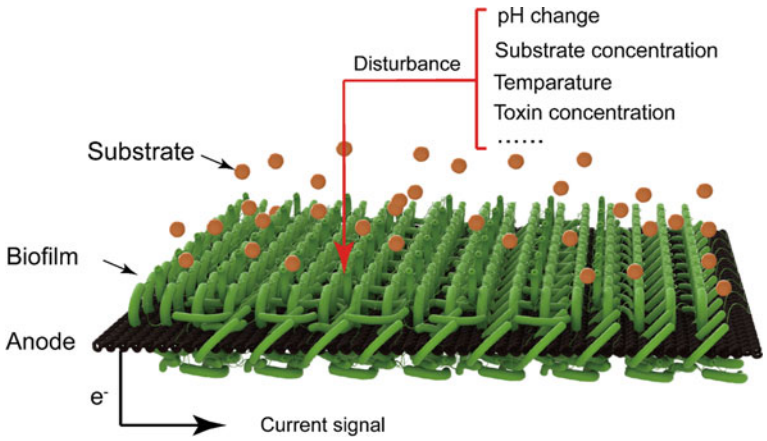

Fig. 18 Schematic of MFC based biosensor

detection, volatile fatty acids and anaerobic digestion processing [140, 142–146]. However, the stability, sensitivity, response time, and detection limit of the biosensor system still need improvement for practical application and to successfully compete with other analytical methods.

7 Outlook

Although MFC technology has been intensively studied as a promising method to achieve sustainable wastewater treatment and electricity generation, many barriers need to be overcome before practical implementation. Among these, fabrication of high-performance and cost-effective anodes and cathodes are the most important challenges. Many alternative anode materials, such as carbon brushes, loofah sponge-derived porous carbon, graphene aerogels, and carbon nanomaterials, have been used in MFCs. These 3D porous electrodes can achieve a higher performance level than carbon cloth/paper because of the greater electrode surface accessible to electroactive bacteria. However, their high price and the complex production process offsets the benefits from the performance improvement. A low-cost and high-performance cathode is equally important for MFC performance. MFCs using carbonaceous materials as the ORR catalysts can deliver similar or greater performance than that of the Pt/C cathode, while the cost can be reduced by at least one order of magnitude. However, fabricating and doping the carbon materials usually requires toxic chemicals, sophisticated preparation routes, and specialized equipment. Preparation of these catalysts can have a negative environmental impact.

Although there has been significant development in MFCs recent years, most of these achievements were based on lab-size MFCs ranging from microliters to milliliters. Therefore, these results cannot be directly applied to large-scale reactors

due to poor understanding of the effects of reactor architecture and operation conditions on MFC performance. In a scaled-up system, water pressure, that is quite low in a lab-scale MFC, can challenge the mechanical strength and the stability of the air-cathode. Additionally, the wastewater usually contains small particles. These may block reactor pipes and limit the substrate supply to the biofilm, leading to a significant decrease of biofilm activity on the anode. Therefore, many efforts are needed to develop or establish an improved MFC system that can be operated in a real wastewater treatment plant.

MFCs represent a proven carbon neutral technology and they can be used for renewable energy production and wastewater treatment. There is a bright and promising future for a wide range of MFC technologies and these are the foundation of a new generation of renewable energy systems.

Acknowledgements This work was supported by National Natural Science Funds for Outstanding Young Scholar (No. 51622602), the National Natural Science Funds for Distinguished Young Scholar (No. 51325602), the National Science Foundation for Young Scientists of China (No. 51506017) and a project supported by the Natural Science Foundation of Chongqing, China (Grant No: cstc2015jcyjA90017).

References

1. Logan BE, Hamelers B, Rozendal R, Schröder U, Keller J, Freguia S, Aelterman P, Verstraete W, Rabaey K (2006) Microbial fuel cells: methodology and technology. Environ Sci Technol 40(17):5181–5192
2. Liu H, Ramnarayanan R, Logan BE (2004) Production of electricity during wastewater treatment using a single chamber microbial fuel cell. Environ Sci Technol 38(7):2281–2285
3. Du Z, Li H, Gu T (2007) A state of the art review on microbial fuel cells: a promising technology for wastewater treatment and bioenergy. Biotechnol Adv 25(5):464–482
4. Pant D, Bogaert GV, Diels L, Diels L (2010) A review of the substrates used in microbial fuel cells (MFCs) for sustainable energy production. Bioresour Technol 101(6):1533–1543
5. Logan BE (2010) Scaling up microbial fuel cells and other bioelectrochemical systems. Appl Microbiol Biot 85(6):1665–1671
6. Dong H, Yu H, Wang X, Zhou Q, Feng J (2012) A novel structure of scalable air-cathode without Nafion and Pt by rolling activated carbon and PTFE as catalyst layer in microbial fuel cells. Water Res 46(17):5777
7. Catal T, Li K, Bermek H, Liu H (2008) Electricity production from twelve monosaccharides using microbial fuel cells. J Power Sources 175(1):196–200
8. Logan B, Cheng S, Watson V, Estadt G (2007) Graphite fiber brush anodes for increased power production in air-cathode microbial fuel cells. Environ Sci Technol 41(9):3341–3346
9. Manohar AK, Mansfeld F (2009) The internal resistance of a microbial fuel cell and its dependence on cell design and operating conditions. Electrochim Acta 54(6):1664–1670
10. Wang X, Feng Y, Ren N, Wang H, Lee H, Li N, Zhao Q (2009) Accelerated start-up of two-chambered microbial fuel cells: effect of anodic positive poised potential. Electrochim Acta 54(3):1109–1114
11. Feng Y, Wang X, Logan BE, Lee H (2008) Brewery wastewater treatment using air-cathode microbial fuel cells. Appl Microbiol Biotechnol 78(5):873–880

12. Wen Q, Wu Y, Cao D, Zhao L, Sun Q (2009) Electricity generation and modeling of microbial fuel cell from continuous beer brewery wastewater. Bioresour Technol 100(18): 4171–4175
13. Lu N, S-g Zhou, Zhuang L, J-t Zhang, J-r Ni (2009) Electricity generation from starch processing wastewater using microbial fuel cell technology. Biochem Eng J 43(3):246–251
14. Greenman J, Gálvez A, Giusti L, Ieropoulos I (2009) Electricity from landfill leachate using microbial fuel cells: comparison with a biological aerated filter. Enzyme Microb Tech 44(2): 112–119
15. Sun J, Y-y Hu, Bi Z, Y-q Cao (2009) Simultaneous decolorization of azo dye and bioelectricity generation using a microfiltration membrane air-cathode single-chamber microbial fuel cell. Bioresour Technol 100(13):3185–3192
16. Jadhav G, Ghangrekar M (2009) Performance of microbial fuel cell subjected to variation in pH, temperature, external load and substrate concentration. Bioresour Technol 100(2): 717–723
17. Chakrapani S, Perozo E (2006) Increased performance of single-chamber microbial fuel cells using an improved cathode structure. Electrochem Commun 8(3):489–494
18. Logan BE (2008) Microbial fuel cells. Wiley
19. He Z, Liu J, Qiao Y, Li CM, Tan TTY (2012) Architecture engineering of hierarchically porous chitosan/vacuum-stripped graphene scaffold as bioanode for high performance microbial fuel cell. Nano Lett 12(9):4738
20. Higgins SR, Foerster D, Cheung A, Lau C, Bretschger O, Minteer SD, Nealson K, Atanassov P, Cooney MJ (2011) Fabrication of macroporous chitosan scaffolds doped with carbon nanotubes and their characterization in microbial fuel cell operation. Enzyme Microb Tech 48(6):458–465
21. Qiao Y, Li CM, Bao S-J, Bao Q-L (2007) Carbon nanotube/polyaniline composite as anode material for microbial fuel cells. J Power Sources 170(1):79–84
22. Manickam SS, Karra U, Huang L, Bui NN, Li B, McCutcheon JR (2013) Activated carbon nanofiber anodes for microbial fuel cells. Carbon 53:19–28
23. Wang H, Wang G, Ling Y, Qian F, Song Y, Lu X, Chen S, Tong Y, Li Y (2013) High power density microbial fuel cell with flexible 3D graphene–nickel foam as anode. Nanoscale 5(21):10283–10290
24. Xie X, Hu L, Pasta M, Wells GF, Kong D, Criddle CS, Cui Y (2011) Three-dimensional carbon nanotube-textile anode for high-performance microbial fuel cells. Nano Lett 11(1): 291–296
25. Xing X, Yu GH, Liu N, Bao ZN, Criddle CS, Yi C (2012) Graphene-sponges as high-performance low-cost anodes for microbial fuel cells. Energy Environ Sci 5(5):6862–6866
26. Yong YC, Dong XC, Chanpark MB, Song H, Chen P (2012) Macroporous and monolithic anode based on polyaniline hybridized three-dimensional graphene for high-performance microbial fuel cells. ACS Nano 6(3):2394
27. ter Heijne A, Hamelers HV, Saakes M, Buisman CJ (2008) Performance of non-porous graphite and titanium-based anodes in microbial fuel cells. Electrochim Acta 53(18):5697–5703
28. Baudler A, Schmidt I, Langner M, Greiner A, Schröder U (2015) Does it have to be carbon? Metal anodes in microbial fuel cells and related bioelectrochemical systems. Energy Environ Sci 8(7):2048–2055
29. Zhang X, Shi J, Liang P, Wei J, Huang X, Zhang C, Logan BE (2013) Power generation by packed-bed air-cathode microbial fuel cells. Bioresour Technol 142:109–114
30. Zhang GD, Zhao QL, Jiao Y, Zhang JN, Jiang JQ, Ren N, Kim BH (2011) Improved performance of microbial fuel cell using combination biocathode of graphite fiber brush and graphite granules. J Power Sources 196(15):6036–6041
31. Zhao F, Rahunen N, Varcoe JR, Chandra A, Avignonerossa C, Thumser AE, Slade RCT (2008) Activated carbon cloth as anode for sulfate removal in a microbial fuel cell. Environ Sci Technol 42(13):4971–4976

32. Zhang L, Li J, Zhu X, Ye D, Liao Q (2013) Anodic current distribution in a liter-scale microbial fuel cell with electrode arrays. Chem Eng J 223(5):623–631
33. Lepage G, Albernaz FO, Perrier G, Merlin G (2012) Characterization of a microbial fuel cell with reticulated carbon foam electrodes. Bioresour Technol 124(337):199–207
34. Yuan Y, Kim SH (2008) Polypyrrole-coated reticulated vitreous carbon as anode in microbial fuel cell for higher energy output. Bull Korean Chem Soc 29(29):168–172
35. Sasaki K, Yasuda K, Nakanishi K, Rakugi H, Isaka Y, Yamato M (2011) Granular activated carbon based microbial fuel cell for simultaneous decolorization of real dye wastewater and electricity generation. New Biotechnol 29(1):32–37
36. Li J, Liu C, Liao Q, Zhu X, Ye D (2013) Improved performance of a tubular microbial fuel cell with a composite anode of graphite fiber brush and graphite granules. Int J Hydrog Energy 38(35):15723–15729
37. Liu C, Li J, Zhu X, Zhang L, Ye D, Brown RK, Liao Q (2013) Effects of brush lengths and fiber loadings on the performance of microbial fuel cells using graphite fiber brush anodes. Int J Hydrog Energy 38(35):15646–15652
38. Katuri K, Ferrer ML, Gutiérrez MC, Jiménez R, del Monte F, Leech D (2011) Three-dimensional microchanelled electrodes in flow-through configuration for bioanode formation and current generation. Energy Environ Sci 4(10):4201–4210
39. Chen S, Liu Q, He G, Zhou Y, Hanif M, Peng X, Wang S, Hou H (2012) Reticulated carbon foam derived from a sponge-like natural product as a high-performance anode in microbial fuel cells. J Mater Chem 22(35):18609–18613
40. Yuan Y, Zhou S, Liu Y, Tang J (2013) Nanostructured macroporous bioanode based on polyaniline-modified natural loofah sponge for high-performance microbial fuel cells. Environ Sci Technol 47(24):14525–14532
41. Zhang J, Li J, Ye D, Zhu X, Liao Q, Zhang B (2014) Tubular bamboo charcoal for anode in microbial fuel cells. J Power Sources 272:277–282
42. Chen Q, Pu W, Hou H, Hu J, Liu B, Li J, Cheng K, Huang L, Yuan X, Yang C (2018) Activated microporous-mesoporous carbon derived from chestnut shell as a sustainable anode material for high performance microbial fuel cells. Bioresour Technol 249:567–573
43. Karthikeyan R, Wang B, Xuan J, Wong JW, Lee PK, Leung MK (2015) Interfacial electron transfer and bioelectrocatalysis of carbonized plant material as effective anode of microbial fuel cell. Electrochim Acta 157:314–323
44. Lu M, Qian Y, Yang C, Huang X, Li H, Xie X, Huang L, Huang W (2016) Nitrogen-enriched pseudographitic anode derived from silk cocoon with tunable flexibility for microbial fuel cells. Nano Energy 32:382–388
45. Ren H, Pyo S, Lee J-I, Park T-J, Gittleson FS, Leung FC, Kim J, Taylor AD, Lee H-S, Chae J (2015) A high power density miniaturized microbial fuel cell having carbon nanotube anodes. J Power Sources 273:823–830
46. Hindatu Y, Annuar M, Gumel A (2017) Mini-review: anode modification for improved performance of microbial fuel cell. Renew Sustain Energy Rev 73:236–248
47. Liu J, Qiao Y, Guo CX, Lim S, Song H, Li CM (2012) Graphene/carbon cloth anode for high-performance mediatorless microbial fuel cells. Bioresour Technol 114:275–280
48. Zhang Y, Mo G, Li X, Zhang W, Zhang J, Ye J, Huang X, Yu C (2011) A graphene modified anode to improve the performance of microbial fuel cells. J Power Sources 196 (13):5402–5407
49. Wang P, Li H, Du Z (2014) Polyaniline synthesis by cyclic voltammetry for anodic modification in microbial fuel cells. Int J Electrochem Sci 9:2038–2046
50. Lv Z, Chen Y, Wei H, Li F, Hu Y, Wei C, Feng C (2013) One-step electrosynthesis of polypyrrole/graphene oxide composites for microbial fuel cell application. Electrochim Acta 111:366–373
51. Gnana Kumar G, Kirubaharan CJ, Udhayakumar S, Ramachandran K, Karthikeyan C, Renganathan R, Nahm KS (2014) Synthesis, structural, and morphological characterizations of reduced graphene oxide-supported polypyrrole anode catalysts for improved microbial fuel cell performances. ACS Sustain Chem Eng 2(10):2283–2290

52. Zhu N, Chen X, Zhang T, Wu P, Li P, Wu J (2011) Improved performance of membrane free single-chamber air-cathode microbial fuel cells with nitric acid and ethylenediamine surface modified activated carbon fiber felt anodes. Bioresour Technol 102(1):422–426
53. Feng Y, Yang Q, Wang X, Logan BE (2010) Treatment of carbon fiber brush anodes for improving power generation in air–cathode microbial fuel cells. J Power Sources 195 (7):1841–1844
54. Cheng S, Logan BE (2007) Ammonia treatment of carbon cloth anodes to enhance power generation of microbial fuel cells. Electrochem Commun 9(3):492–496
55. Zhang J, Li J, Ye D, Zhu X, Liao Q, Zhang B (2014) Enhanced performances of microbial fuel cells using surface-modified carbon cloth anodes: a comparative study. Int J Hydrog Energy 39(33):19148–19155
56. Zhou M, Chi M, Wang H, Jin T (2012) Anode modification by electrochemical oxidation: a new practical method to improve the performance of microbial fuel cells. Biochem Eng J 60:151–155
57. Mauritz KA, Moore RB (2004) State of understanding of Nafion. Chem Rev 104(10):4535–4586
58. Nambiar S, Togo C, Limson J (2009) Application of multi-walled carbon nanotubes to enhance anodic performance of an Enterobacter cloacae-based fuel cell. Afr J Biotechnol 8(24)
59. Pant D, Van Bogaert G, De Smet M, Diels L, Vanbroekhoven K (2010) Use of novel permeable membrane and air cathodes in acetate microbial fuel cells. Electrochim Acta 55 (26):7710–7716
60. Leong JX, Daud WRW, Ghasemi M, Liew KB, Ismail M (2013) Ion exchange membranes as separators in microbial fuel cells for bioenergy conversion: a comprehensive review. Renew Sustain Energy Rev 28:575–587
61. Zaidi SJ, Mikhailenko SD, Robertson G, Guiver M, Kaliaguine S (2000) Proton conducting composite membranes from polyether ether ketone and heteropolyacids for fuel cell applications. J Membr Sci 173(1):17–34
62. Zhang X, Cheng S, Huang X, Logan BE (2010) Improved performance of single-chamber microbial fuel cells through control of membrane deformation. Biosens Bioelectron 25 (7):1825–1828
63. Kazemi S, Fatih K, Mohseni M, Wang H (2012) Investigating separators to improve performance of flat-plate microbial fuel cells. Meeting Abstracts: The Electrochemical Society, pp 3593–3593
64. Kim JR, Cheng S, Oh S-E, Logan BE (2007) Power generation using different cation, anion, and ultrafiltration membranes in microbial fuel cells. Environ Sci Technol 41(3):1004–1009
65. Sun J, Hu Y, Bi Z, Cao Y (2009) Improved performance of air-cathode single-chamber microbial fuel cell for wastewater treatment using microfiltration membranes and multiple sludge inoculation. J Power Sources 187(2):471–479
66. Yang W, Li J, Zhang L, Zhu X, Liao Q (2017) A monolithic air cathode derived from bamboo for microbial fuel cells. RSC Adv 7(45):28469–28475
67. Zhang X, Cheng S, Huang X, Logan BE (2010) The use of nylon and glass fiber filter separators with different pore sizes in air-cathode single-chamber microbial fuel cells. Energy Environ Sci 3(5):659–664
68. Fan Y, Hu H, Liu H (2007) Enhanced Coulombic efficiency and power density of air-cathode microbial fuel cells with an improved cell configuration. J Power Sources 171(2): 348–354
69. Li J, Fu Q, Liao Q, Zhu X, D-d Ye, Tian X (2009) Persulfate: a self-activated cathodic electron acceptor for microbial fuel cells. J Power Sources 194(1):269–274
70. Zhang L, Zhu X, Li J, Liao Q, Ye D (2011) Biofilm formation and electricity generation of a microbial fuel cell started up under different external resistances. J Power Sources 196 (15):6029–6035
71. Cheng S, Liu H, Logan BE (2006) Power densities using different cathode catalysts (Pt and CoTMPP) and polymer binders (Nafion and PTFE) in single chamber microbial fuel cells. Environ Sci Technol 40(1):364–369

72. Zhang F, Cheng S, Pant D, Van Bogaert G, Logan BE (2009) Power generation using an activated carbon and metal mesh cathode in a microbial fuel cell. Electrochem Commun 11 (11):2177–2179
73. Yang W, Li J, Ye D, Zhu X, Liao Q (2017) Bamboo charcoal as a cost-effective catalyst for an air-cathode of microbial fuel cells. Electrochim Acta 224:585–592
74. Watson VJ, Nieto Delgado C, Logan BE (2013) Influence of chemical and physical properties of activated carbon powders on oxygen reduction and microbial fuel cell performance. Environ Sci Technol 47(12):6704–6710
75. Zhou L, Fu P, Wen D, Yuan Y, Zhou S (2016) Self-constructed carbon nanoparticles-coated porous biocarbon from plant moss as advanced oxygen reduction catalysts. Appl Catal B-Environ 181:635–643
76. Liu L, Xiong Q, Li C, Feng Y, Chen S (2015) Conversion of straw to nitrogen doped carbon for efficient oxygen reduction catalysts in microbial fuel cells. RSC Adv 5(109):89771–89776
77. Sun Y, Duan Y, Hao L, Xing Z, Dai Y, Li R, Zou J (2016) Cornstalk-derived nitrogen-doped partly graphitized carbon as efficient metal-free catalyst for oxygen reduction reaction in microbial fuel cells. ACS Appl Mater Inter 8(39):25923–25932
78. Wang H, Zhang Z, Yang Y, Wang K, Ji S, Key J, Ma Y, Wang R (2015) A Co-N-doped carbonized egg white as a high-performance, non-precious metal, electrocatalyst for oxygen reduction. J Solid State Electron 19(6):1727–1733
79. Wu H, Geng J, Ge H, Guo Z, Wang Y, Zheng G (2016) Egg-derived mesoporous carbon microspheres as bifunctional oxygen evolution and oxygen reduction electrocatalysts. Adv Energy Mater 6(20)
80. Fan Z, Li J, Zhou Y, Fu Q, Yang W, Zhu X, Liao Q (2017) A green, cheap, high-performance carbonaceous catalyst derived from Chlorella pyrenoidosa for oxygen reduction reaction in microbial fuel cells. Int J Hydrog Energy
81. Deng L, Yuan H, Cai X, Ruan Y, Zhou S, Chen Y, Yuan Y (2016) Honeycomb-like hierarchical carbon derived from livestock sewage sludge as oxygen reduction reaction catalysts in microbial fuel cells. Int J Hydrog Energy 41(47):22328–22336
82. Yuan Y, Liu T, Fu P, Tang J, Zhou S (2015) Conversion of sewage sludge into high-performance bifunctional electrode materials for microbial energy harvesting. J Mater Chem A 3(16):8475–8482
83. Dong H, Yu H, Wang X, Zhou Q, Feng J (2012) A novel structure of scalable air-cathode without Nafion and Pt by rolling activated carbon and PTFE as catalyst layer in microbial fuel cells. Water Res 46(17):5777–5787
84. Dong H, Yu H, Yu H, Gao N, Wang X (2013) Enhanced performance of activated carbon–polytetrafluoroethylene air-cathode by avoidance of sintering on catalyst layer in microbial fuel cells. J Power Sources 232:132–138
85. Yang W, He W, Zhang F, Hickner MA, Logan BE (2014) Single-step fabrication using a phase inversion method of poly (vinylidene fluoride)(PVDF) activated carbon air cathodes for microbial fuel cells. Environ Sci Technol Lett 1(10):416–420
86. Cheng S, Wu J (2013) Air-cathode preparation with activated carbon as catalyst, PTFE as binder and nickel foam as current collector for microbial fuel cells. Bioelectrochemistry 92:22–26
87. Popat SC, Ki D, Rittmann BE, Torres CI (2012) Importance of OH^- transport from cathodes in microbial fuel cells. ChemSusChem 5(6):1071–1079
88. Popat SC, Ki D, Young MN, Rittmann BE, Torres CI (2014) Buffer pKa and transport govern the concentration over potential in electrochemical oxygen reduction at neutral pH. ChemElectroChem 1(11):1909–1915
89. Liu H, Cheng S, Logan BE (2005) Production of electricity from acetate or butyrate using a single-chamber microbial fuel cell. Environ Sci Technol 39(2):658–662
90. Li X, Wang X, Zhang Y, Ding N, Zhou Q (2014) Opening size optimization of metal matrix in rolling-pressed activated carbon air–cathode for microbial fuel cells. Appl Energy 123:13–18

91. You S, Zhao Q, Zhang J, Jiang J, Zhao S (2006) A microbial fuel cell using permanganate as the cathodic electron acceptor. J Power Sources 162(2):1409–1415
92. Li J, Fu Q, Zhu X, Liao Q, Zhang L, Wang H (2010) A solar regenerable cathodic electron acceptor for microbial fuel cells. Electrochim Acta 55(7):2332–2337
93. Tartakovsky B, Guiot SR (2006) A comparison of air and hydrogen peroxide oxygenated microbial fuel cell reactors. Biotechnol Progr 22(1):241–246
94. Tang X, Li H, Du Z, Wang W, Ng HY (2015) Conductive polypyrrole hydrogels and carbon nanotubes composite as an anode for microbial fuel cells. Rsc Adv 5(63):50968–50974
95. Min B, Cheng S, Logan BE (2005) Electricity generation using membrane and salt bridge microbial fuel cells. Water Res 39(9):1675–1686
96. Min B, Logan BE (2004) Continuous electricity generation from domestic wastewater and organic substrates in a flat plate microbial fuel cell. Environ Sci Technol 38(21):5809–5814
97. Liu H, Logan BE (2004) Electricity generation using an air-cathode single chamber microbial fuel cell in the presence and absence of a proton exchange membrane. Environ Sci Technol 38(14):4040–4046
98. Cheng S, Logan BE (2011) Increasing power generation for scaling up single-chamber air cathode microbial fuel cells. Bioresour Technol 102(6):4468–4473
99. Call DF, Logan BE (2011) A method for high throughput bioelectrochemical research based on small scale microbial electrolysis cells. Biosens Bioelectron 26(11):4526–4531
100. Cristiani P, Franzetti A, Gandolfi I, Guerrini E, Bestetti G (2013) Bacterial DGGE fingerprints of biofilms on electrodes of membraneless microbial fuel cells. Int Biodeterior Biodegrad 84:211–219
101. Janicek A, Fan Y, Liu H (2014) Design of microbial fuel cells for practical application: a review and analysis of scale-up studies. Biofuels 5(1):79–92
102. Kim JR, Premier GC, Hawkes FR, Dinsdale RM, Guwy AJ (2009) Development of a tubular microbial fuel cell (MFC) employing a membrane electrode assembly cathode. J Power Sources 187(2):393–399
103. Kim JR, Rodríguez J, Hawkes FR, Dinsdale RM, Guwy AJ, Premier GC (2011) Increasing power recovery and organic removal efficiency using extended longitudinal tubular microbial fuel cell (MFC) reactors. Energy Environ Sci 4(2):459–465
104. Zhuang L, Zhou S (2009) Substrate cross-conduction effect on the performance of serially connected microbial fuel cell stack. Electrochem Commun 11(5):937–940
105. Cheng S, Liu H, Logan BE (2006) Increased performance of single-chamber microbial fuel cells using an improved cathode structure. Electrochem Commun 8(3):489–494
106. Qiu Z, Su M, Wei L, Han H, Jia Q, Shen J (2015) Improvement of microbial fuel cell cathodes using cost-effective polyvinylidene fluoride. J Power Sources 273:566–573
107. Santoro C, Agrios A, Pasaogullari U, Li B (2011) Effects of gas diffusion layer (GDL) and micro porous layer (MPL) on cathode performance in microbial fuel cells (MFCs). Int J Hydrog Energy 36(20):13096–13104
108. Zhang Y, Wang X, Li X, Gao N, Wan L, Feng C, Zhou Q (2014) A novel and high performance activated carbon air-cathode with decreased volume density and catalyst layer invasion for microbial fuel cells. RSC Adv 4(80):42577–42580
109. Li D, Qu Y, Liu J, He W, Wang H, Feng Y (2014) Using ammonium bicarbonate as pore former in activated carbon catalyst layer to enhance performance of air cathode microbial fuel cell. J Power Sources 272:909–914
110. Yang W, Logan BE (2016) Engineering a membrane based air cathode for microbial fuel cells via hot pressing and using multi-catalyst layer stacking. Environ Sci: Water Res Technol 2(5):858–863
111. Yang G, Erbay C, S-i Yi, de Figueiredo P, Sadr R, Han A, Yu C (2016) Bifunctional nano-sponges serving as non-precious metal catalysts and self-standing cathodes for high performance fuel cell applications. Nano Energy 22:607–614
112. Wu Z-S, Yang S, Sun Y, Parvez K, Feng X, Müllen K (2012) 3D nitrogen-doped graphene aerogel-supported Fe_3O_4 nanoparticles as efficient electrocatalysts for the oxygen reduction reaction. J Am Chem Soc 134(22):9082–9085

113. Wu S, Li H, Zhou X, Liang P, Zhang X, Jiang Y, Huang X (2016) A novel pilot-scale stacked microbial fuel cell for efficient electricity generation and wastewater treatment. Water Res 98:396–403
114. Aelterman P, Rabaey K, Pham HT, Boon N, Verstraete W (2006) Continuous electricity generation at high voltages and currents using stacked microbial fuel cells. Environ Sci Technol 40(10):3388–3394
115. Gurung A, Oh S-E (2012) The performance of serially and parallelly connected microbial fuel cells. Energy Sources Part A: Recovery Util Environ Effects 34(17):1591–1598
116. Ieropoulos IA, Ledezma P, Stinchcombe A, Papaharalabos G, Melhuish C, Greenman J (2013) Waste to real energy: the first MFC powered mobile phone. Phys Chem Chem Phys 15(37):15312–15316
117. Zhuang L, Zheng Y, Zhou S, Yuan Y, Yuan H, Chen Y (2012) Scalable microbial fuel cell (MFC) stack for continuous real wastewater treatment. Bioresour Technol 106:82–88
118. Yousefi V, Mohebbi-Kalhori D, Samimi A, Salari M (2016) Effect of separator electrode assembly (SEA) design and mode of operation on the performance of continuous tubular microbial fuel cells (MFCs). Int J Hydrog Energy 41(1):597–606
119. Ieropoulos IA, Greenman J, Melhuish C (2013) Miniature microbial fuel cells and stacks for urine utilisation. Int J Hydrog Energy 38(1):492–496
120. Ren L, Ahn Y, Hou H, Zhang F, Logan BE (2014) Electrochemical study of multi-electrode microbial fuel cells under fed-batch and continuous flow conditions. J Power Sources 257:454–460
121. Miyahara M, Hashimoto K, Watanabe K (2013) Use of cassette-electrode microbial fuel cell for wastewater treatment. J Biosci Bioeng 115(2):176–181
122. Ledezma P, Stinchcombe A, Greenman J, Ieropoulos I (2013) The first self-sustainable microbial fuel cell stack. Phys Chem Chem Phys 15(7):2278–2281
123. Oh S-E, Logan BE (2007) Voltage reversal during microbial fuel cell stack operation. J Power Sources 167(1):11–17
124. An J, Lee HS (2014) Occurrence and implications of voltage reversal in stacked microbial fuel cells. ChemSusChem 7(6):1689–1695
125. An J, Kim B, Chang IS, Lee H-S (2015) Shift of voltage reversal in stacked microbial fuel cells. J Power Sources 278:534–539
126. Wu PK, Biffinger JC, Fitzgerald LA, Ringeisen BR (2012) A low power DC/DC booster circuit designed for microbial fuel cells. Process Biochem 47(11):1620–1626
127. Boghani HC, Papaharalabos G, Michie I, Fradler KR, Dinsdale RM, Guwy AJ, Ieropoulos I, Greenman J, Premier GC (2014) Controlling for peak power extraction from microbial fuel cells can increase stack voltage and avoid cell reversal. J Power Sources 269:363–369
128. An J, Sim J, Lee H-S (2015) Control of voltage reversal in serially stacked microbial fuel cells through manipulating current: significance of critical current density. J Power Sources 283:19–23
129. Kim Y, Hatzell MC, Hutchinson AJ, Logan BE (2011) Capturing power at higher voltages from arrays of microbial fuel cells without voltage reversal. Energy Environ Sci 4(11):4662–4667
130. Khaled F, Ondel O, Allard B, Degrenne N (2013) Voltage balancing circuit for energy harvesting from a stack of serially-connected microbial fuel cells. In: 2013 IEEE ECCE Asia Downunder (ECCE Asia). IEEE, pp 392–397
131. Yang W, Li J, Ye D, Zhang L, Zhu X, Liao Q (2016) A hybrid microbial fuel cell stack based on single and double chamber microbial fuel cells for self-sustaining pH control. J Power Sources 306:685–691
132. Andersen SJ, Pikaar I, Freguia S, Lovell BC, Rabaey K, Rozendal RA (2013) Dynamically adaptive control system for bioanodes in serially stacked bioelectrochemical systems. Environ Sci Technol 47(10):5488–5494
133. Kim B, Lee BG, Kim BH, Chang IS (2015) Assistance current effect for prevention of voltage reversal in stacked microbial fuel cell systems. ChemElectroChem 2(5):755–760

134. Wang A, Sun D, Cao G, Wang H, Ren N, Wu W-M, Logan BE (2011) Integrated hydrogen production process from cellulose by combining dark fermentation, microbial fuel cells, and a microbial electrolysis cell. Bioresour Technol 102(5):4137–4143
135. Sun M, Sheng G-P, Zhang L, Xia C-R, Mu Z-X, Liu X-W, Wang H-L, Yu H-Q, Qi R, Yu T (2008) An MEC-MFC-coupled system for biohydrogen production from acetate. Environ Sci Technol 42(21):8095–8100
136. Mohanakrishna G, Mohan SV, Sarma P (2010) Utilizing acid-rich effluents of fermentative hydrogen production process as substrate for harnessing bioelectricity: an integrative approach. Int J Hydrogen Energ 35(8):3440–3449
137. Vazquez-Larios AL, Solorza-Feria O, Vazquez-Huerta G, Esparza-García F, Rinderknecht-Seijas N, Poggi-Varaldo HM (2011) Effects of architectural changes and inoculum type on internal resistance of a microbial fuel cell designed for the treatment of leachates from the dark hydrogenogenic fermentation of organic solid wastes. Int J Hydrog Energy 36(10):6199–6209
138. Li J, Zou W, Xu Z, Ye D, Zhu X, Liao Q (2013) Improved hydrogen production of the downstream bioreactor by coupling single chamber microbial fuel cells between series-connected photosynthetic biohydrogen reactors. Int J Hydrog Energy 38(35): 15613–15619
139. Huang L, Yao B, Wu D, Quan X (2014) Complete cobalt recovery from lithium cobalt oxide in self-driven microbial fuel cell–microbial electrolysis cell systems. J Power Sources 259:54–64
140. Stein NE, Hamelers HV, Buisman CN (2012) The effect of different control mechanisms on the sensitivity and recovery time of a microbial fuel cell based biosensor. Sens Actuators B: Chem 171:816–821
141. Di Lorenzo M, Curtis TP, Head IM, Scott K (2009) A single-chamber microbial fuel cell as a biosensor for wastewaters. Water Res 43(13):3145–3154
142. Stein NE, Hamelers HV, Buisman CN (2010) Stabilizing the baseline current of a microbial fuel cell-based biosensor through over potential control under non-toxic conditions. Bioelectrochemistry 78(1):87–91
143. Kim BH, Chang IS, Gil GC, Park HS, Kim HJ (2003) Novel BOD (biological oxygen demand) sensor using mediator-less microbial fuel cell. Biotechnol Lett 25(7):541–545
144. Donovan C, Dewan A, Heo D, Beyenal H (2008) Batteryless, wireless sensor powered by a sediment microbial fuel cell. Environ Sci Technol 42(22):8591–8596
145. Stein NE, Hamelers HM, van Straten G, Keesman KJ (2012) On-line detection of toxic components using a microbial fuel cell-based biosensor. J Process Control 22(9):1755–1761
146. Kaur A, Kim JR, Michie I, Dinsdale RM, Guwy AJ, Premier GC (2013) Microbial fuel cell type biosensor for specific volatile fatty acids using acclimated bacterial communities. Biosens Bioelectron 47:50–55